

University of Mississippi

eGrove

---

Electronic Theses and Dissertations

Graduate School

---

1-1-2022

# APPLICATION OF HOT-MELT EXTRUSION AND FUSED DEPOSITION MODELING ON SCREENING FILAMENTS AND DEVELOPING DIVERSE DOSAGES

Pengchong Xu

Follow this and additional works at: <https://egrove.olemiss.edu/etd>

---

## Recommended Citation

Xu, Pengchong, "APPLICATION OF HOT-MELT EXTRUSION AND FUSED DEPOSITION MODELING ON SCREENING FILAMENTS AND DEVELOPING DIVERSE DOSAGES" (2022). *Electronic Theses and Dissertations*. 2297.

<https://egrove.olemiss.edu/etd/2297>

This Dissertation is brought to you for free and open access by the Graduate School at eGrove. It has been accepted for inclusion in Electronic Theses and Dissertations by an authorized administrator of eGrove. For more information, please contact [egrove@olemiss.edu](mailto:egrove@olemiss.edu).

APPLICATION OF HOT-MELT EXTRUSION AND FUSED  
DEPOSITION MODELING ON SCREENING FILAMENTS AND  
DEVELOPING DIVERSE DOSAGES

A Dissertation  
presented in partial fulfillment of requirements  
for the Doctoral of Philosophy in Pharmaceutical Sciences  
in the Department of Pharmaceutics and Drug Delivery  
The University of Mississippi

by

PENGCHONG XU

May 2022

Copyright Pengchong Xu 2022

ALL RIGHTS RESERVE

## ABSTRACT

Three-dimensional printing (3DP) provides a flexible and cost-beneficial solution to patient-centric medicine and its potential to challenge current pharmaceutical supply chains. Fusion deposition modeling (FDM) is one of the most commonly applied 3D printing techniques in pharmaceutical study. But the poor mechanical properties of printing filaments have limited mainly the application of FDM 3D printing in the pharmaceutical area.

In this dissertation, the development of texture analysis methods to evaluate the printability of filaments was investigated first. The parameter “Stiffness” was successfully developed to measure and predict the printability of filaments in the direct-extrude FDM printer. Then, the combination of hot-melt extrusion (HME) and 3DP technologies was applied to fabricate 16 kinds of tablets with different geometries and polymer matrices. Release kinetics and correlation between the mean dissolution time (MDT) and surface area to volume (SA/V) ratio were studied. A comprehensive understanding of the influence of different structures and matrices on drug release was obtained. Finally, Two-APIs pulsatile release tablets were successfully produced by FDM and HME technologies. The correlation between the thickness of the first layer and the second drug release time was also studied, and a good correlation was obtained.

## LIST OF ABBREVIATIONS

AM	Additive manufacturing	HPMCAS	Hypromellose acetate
API	Active pharmaceutical ingredients		succinate
		PDDS	Pulsatile drug delivery system
APAP	Acetaminophen	PLA	Polylactic acid
ASD	Amorphous solid dispersion	PVA	Polyvinyl alcohol
BCS	Biopharmaceutics Classification System	PVP	Polyvinylpyrrolidone
		SEM	Scanning electronic
CAD	Computer-aided design		microscopy
DDS	Drug delivery systems	TGA	Thermogravimetric analysis
DSC	Differential scanning calorimetry	USP	United States Pharmacopeia
		3DP	3D-printed
FDA	Food and Drug Administration	3PB	Three-point bend
FDM	Fused deposition modeling		
HME	Hot-melt extrusion		
HPLC	High-Performance Liquid Chromatography		
HPMC	Hydroxypropyl methylcellulose		

## ACKNOWLEDGMENT

Throughout the writing of this dissertation, I have received a great deal of support and assistance.

I would first like to thank my advisor, Professor Michael A. Repka, whose expertise was invaluable in small molecule drug delivery. Your insightful feedback pushed me to sharpen my thinking and brought my work to a higher level. You are the best advisor and mentor for my Ph.D. study.

I would like to acknowledge my colleagues from my internship for their wonderful collaboration. I would particularly like to single out my supervisor at Biogen, Xi Zhan, I want to thank you for your patient support and for all of the opportunities I was given to further my research.

I would also like to thank my committee members, Prof. Chalet Tan, Prof. Soumyajit Majumdar, and Prof. Samir Anis Ross, for their valuable guidance throughout my studies.

I want to thank all my friends and lab mates, for their company and help in academic research and life, and for all the good times we had in the last six years.

In addition, I would like to thank my parents for their support and help all the time, encouraging me all the time. It is their support that makes me indomitable and brave the wind and waves on my learning path.

## TABLE OF CONTENTS

ABSTRACT.....	ii
LIST OF ABBREVIATIONS.....	iii
ACKNOWLEDGMENT.....	iv
LIST OF TABLES.....	ix
LIST OF FIGURES.....	x
INTRODUCTION.....	1
CHAPTER I.....	3
1.1. Introduction.....	3
1.2. Materials and Methods.....	5
1.2.1. Materials.....	5
1.2.2. Hot Melt Extrusion and Filament Fabrication.....	6
1.2.3. Differential Scanning Calorimetry (DSC).....	7
1.2.4. Mechanical Characterization of Filaments.....	7
1.2.5. 3D Printer Setup and Printability Test.....	12
1.2.6. Oral Tablet Characterization.....	13
1.2.7. Dissolution.....	13
1.3. Results.....	14
1.3.1. Polymers Behavior in HME and Filament Printability Test in FDM 3D printing.....	14

1.3.2. Comparison of Three Texture Characterization Method and Identification of Toughness .....	19
1.3.3. Characterization and Dissolution of 3D Printed Tablets Using Filaments with Different Toughness Values .....	24
1.4. Discussion .....	27
1.5. Conclusion .....	33
CHAPTER II.....	34
2.1. Introduction.....	34
2.2. Materials and Methods.....	36
2.2.1. Materials .....	36
2.2.2. Formulation.....	36
2.2.3. Hot Melt Extrusion and Filament Fabrication .....	37
2.2.4. Differential Scanning Calorimetry (DSC) .....	37
2.2.5. Thermogravimetric analysis (TGA).....	37
2.2.6. Mechanical characterization of filaments .....	38
2.2.7. Design of 3D geometry models .....	38
2.2.8. 3D printing.....	40
2.2.9. Tablet characterization.....	41
2.2.10. <i>In vitro</i> drug release study.....	41
2.2.11. Mathematical description and release models .....	41
2.3. Results and Discussion .....	44



2.3.1. Preliminary study of raw materials .....	44
2.3.2. Characterization of filaments .....	45
2.3.3. Mechanical Characterization of the Filaments .....	47
2.3.4. Tablet morphology study .....	48
2.3.5. <i>In vitro</i> drug release .....	50
2.4. Conclusion .....	58
CHAPTER III .....	60
3.1 Introduction.....	60
3.2 Materials and Methods.....	62
3.2.1. Materials .....	62
3.2.2. Formulation and preparation of filaments.....	62
3.2.3. Thermogravimetric analysis (TGA).....	63
3.2.4. Differential scanning calorimetry (DSC).....	63
3.2.5. Mechanical characterization of filaments .....	63
3.2.6. Design of 3D models .....	64
3.2.7. 3D printing .....	64
3.2.8. Assessment of tablet morphology .....	65
3.2.9. <i>In vitro</i> drug release study.....	65
3.3 Results and Discussion .....	66
3.3.1. Preliminary study of raw materials .....	66
3.3.2. Characterization of filaments .....	67

3.3.3. Tablet morphology study .....	68
3.3.4. <i>In vitro</i> drug release study.....	68
3.4 Conclusion .....	71
CONCLUSION.....	72
References.....	73
VITA.....	86

## LIST OF TABLES

<b>Table 1.1.</b> Characterization and printability of in-house manufactured filaments.....	16
<b>Table 1.2.</b> Toughness, resistance and brittleness value of in-house filaments using texture analysis methods. ....	22
<b>Table 2.1.</b> Operation parameters for the two different formulations during HME process.	37
<b>Table 2.2.</b> Geometric parameter of each tablet. ....	39
<b>Table 2.3.</b> The parameters of 3D printing process. ....	40
<b>Table 2.4.</b> Characterization of the diffusion exponent $n$ depending on the dosage form geometry. ....	42
<b>Table 2.5.</b> Texture analysis data of three filaments.....	47
<b>Table 2.6.</b> Geometric characteristics of the 3D printed tablets. ....	49
<b>Table 2.7.</b> MDT and SA/V ratio of each tablet. ....	51
<b>Table 3.2.</b> The parameters of each layer of three tablets.....	64
<b>Table 3.3.</b> The parameters of 3D printing process. ....	65
<b>Table 3.4.</b> Texture analysis data of three filaments.....	67
<b>Table 3.5.</b> Geometry study of the tablets. ....	68

## LIST OF FIGURES

<b>Figure 1.1.</b> Illustration of different issues of filaments during printing. a) Brittle filament; b) Soft filament; c) Soft surface. ....	5
<b>Figure 1.2.</b> Standard hot melt extruder configuration.....	7
<b>Figure 1.3.</b> Texture analyzer setup for filament mechanical property test a) Illustration of three-point bend test b) Illustration of Resistance test. c) Illustration of stiffness test. ....	10
<b>Figure 1.4.</b> Texture analysis plots a) Three-point bend test b) Resistance test c) Stiffness test. ....	11
<b>Figure 1.5.</b> Thermogravimetric Analysis of Indomethacin.....	13
<b>Figure 1.6.</b> Differential Thermal Analysis of Indomethacin filaments used in the tablet printing and dissolution experiments. The formulations of filaments are PVPVA-IND4, 15LV-IND2 and .....	15
<b>Figure 1.7.</b> Representative measurements of filament in 3PB test (a, 10 measurements), Resistance test (b, 5 measurements) and Stiffness test (c, 10 measurements).....	21
<b>Figure 1.8.</b> Correlation between the filament printability and the toughness, brittleness, resistance values measured by a) three-bend test, b) resistance test, c) stiffness test, respectively. ....	26
<b>Figure 1.10.</b> Comparison of filament printability evaluation using max force and toughness values in 3PB test and Stiffness test, respectively. ....	30
<b>Figure 1.11.</b> The Printability and Toughness evaluation of Indomethacin/HPMC K15M filament with various plasticizers .....	30

<b>Figure 1.12.</b> Two types of FDM 3D printers and commercial 3D printer examples. a) Direct extrusion; b) Bowden extrusion. ....	32
<b>Figure 2.3.</b> DSC analysis of individual polymers, extruded filaments. ....	45
<b>Figure 2.4.</b> Photos and SEM images of F1 filament (left), F2 filament (middle) and PLA filament (right). ....	46
<b>Figure 2.5.</b> Photos of covers after dissolution test. ....	48
<b>Figure 2.6.</b> Photos of sixteen different structure tablets. ....	49
<b>Figure 2.7.</b> Dissolution profiles of different formulation and structure tablets with or without covers. ....	50
<b>Figure 2.8.</b> Dissolution profiles of same structure tablets with or without covers. ....	51
<b>Figure 2.9.</b> Correlation of MDT and SA/V ratio for F1 and F2 formulation (a, c) and linearized version (b, d). ....	53
<b>Figure 2.10.</b> Plots of drug release rate change during the dissolution process, F1 (a), F2 (b). ....	56
<b>Figure 3.1.</b> The 3D designed models of pulsatile-released tablets. a) 1:1:1:1 ratio of volume; b) 2:2:1:1 ratio of volume (outside in); c) 4:2:2:1 ratio of volume.....	64
<b>Figure 3.2.</b> Thermal degradation graph of the APAP and polymer excipients. ....	66
<b>Figure 3.3.</b> DSC analysis of API, physical mixture, extruded filament.....	67
<b>Figure 3.5.</b> Correlation of start release time of CC and thickness of the first layer (a) and linearized version (b). ....	69
<b>Figure 3.6.</b> Release rate of each tablet during the dissolution test.....	70

## INTRODUCTION

Oral drug administration is generally considered the most convenient and cost-effective drug delivery route for pharmaceuticals and has high patient compliance<sup>1</sup>. However, the development of a new oral drug is time-consuming and expensive. Improving the safety and efficacy ratio of "old drug" is one of the directions of current drug delivery studies. Drug delivery systems (DDSs) are methods or procedures for administering compounds to achieve therapeutic effects in humans or animals. DDSs can improve the efficacy and safety of "old drugs" by controlling the body's speed, timing, and target of drug release to ensure optimal drug distribution and absorption. Practical DDSs approaches include controlled-release agents, where the drug is released at a controlled rate over a period of time, and targeted delivery, where the drug is only effective in a targeted area of the body, such as cancerous tissue<sup>2</sup>.

Additive manufacturing (AM) is a layer-by-layer production of three-dimensional (3D) objects with the help of digital designs<sup>3</sup>. AM equipment and materials were developed in the early 1980s, mainly for chemistry, optics, and robotics research<sup>4</sup>. The first powder-based free-form fabrication using 3D printing methods became available in 1993 at the Massachusetts Institute of Technology (MIT)<sup>5</sup>, in which a standard inkjet head was used to print binders onto loose powders in a powder bed. 3D printing has the potential to disrupt and change the pharmaceutical industry's production model by enabling on-demand customization of personalized medicine. The dose, size, shape, color, taste, and release profile can be adjusted in personalization<sup>6</sup>. Fusion deposition modeling (FDM) is one of the most commonly applied 3D printing techniques in pharmaceutical

study<sup>7</sup>. For pharmaceutical applications of FDM, hot-melt extrusion (HME) can incorporate a drug into the filament<sup>8</sup>. HME is also the best choice for developing pharmaceutical solid dispersions because it is free of using organic solvent and suitable for continuous processing, ensuring optimal quality control<sup>9,10</sup>. However, poor mechanical properties of drug-loaded filaments limited the potential of FDM 3D printing in the pharmaceutical area.

In this dissertation, HME and 3D printing technologies were combined to evaluate the printability of filaments and develop highly personalized or customized tablets. In 1<sup>st</sup> chapter, a series of texture analysis methods were conducted to evaluate the mechanical properties of filaments and try to figure out a parameter that can present the printability of filament in the direct-extrude FDM 3D printer. In the 2<sup>nd</sup> chapter, the relationship between tablets' drug release profiles and different geometries and waterproof covers. Release kinetics and correlation between the mean dissolution time (MDT) and surface area to volume ratio (SA/V) ratio were studied, and a comprehensive understanding of the influence of different structures and matrices on drug release was obtained. In the 3<sup>rd</sup> chapter, the two-APIs pulsatile release tablets were tried to fabricate by HME and FDM technologies. And the dissolution profiles of pulsatile release were tried to adjust by 3D printing technology.

## **CHAPTER I**

### **DEVELOPMENT OF A QUANTITATIVE METHOD TO EVALUATE THE PRINTABILITY OF FILAMENTS FOR FUSED DEPOSITION MODELING 3D PRINTING**

#### **1.1. Introduction**

Oral drug administration is generally considered the most convenient and cost-effective drug delivery route for pharmaceuticals <sup>11,12</sup> and has high patient compliance. In recent years, the interest in applying three-dimensional printing (3DP) in the healthcare industry has been dramatically increased due to its ability to provide a flexible and cost-beneficial solution to patient-centric medicine and its potential to challenge current pharmaceutical supply chains<sup>13</sup>. Unlike the conventional manufacturing process, the 3D printing process, also called additive manufacturing, builds a three-dimensional object by adding layers of material based on the computer-aided design (CAD) model. The first 3D printed orally disintegrating tablet, Spritam®, was launched in 2016 to treat epilepsy in the pharmaceutical industry.

Fused deposition modeling (FDM) is a method of additive manufacturing where layers of materials are fused in a pattern to create an object. FDM systems use solid, polymeric filaments. A gear system drives the filament into the hot end of a print nozzle. The filament is fused in the hot end and pushed out from the nozzle onto the print bed layer by layer <sup>14</sup>. Given the advantages of inexpensive equipment, greater mechanical property diversity, and a higher degree of geometrical freedom of the printed object, the FDM system is, by far, the most popular 3D printing system and is used by nearly half of 3D printing processes<sup>13</sup>.



For pharmaceutical applications of FDM, there are two methods to incorporate a drug into the filament, impregnation and hot-melt extrusion (HME)<sup>15</sup>. Unlike the low drug loading filament produced by the impregnation method<sup>16</sup>, the filament fabricated by HME can achieve relatively higher loading since it applies heat and pressure to melt and mix drug and polymer in a continuous process<sup>17</sup>. The biodegradable polymer is broadly used to stabilize amorphous drugs and enhance bioavailability<sup>18,19</sup>. Compared to traditional pharmaceutical manufacturing methods, the combination of HME and FDM integrates the advantages of both technologies. It has excellent potential to make on-demand manufacturing of patient-centric medicine with improved bioavailability and complex design<sup>13,20-22</sup>.

However, there are still many roadblocks to applying FDM and other 3D printing technologies in the pharmaceutical industry, including technical challenges such as poor filament properties, low printing speed, and quality and regulatory challenges. The mechanical properties limited the application of drug-loaded filament on conventional FDM printers and have been recognized as a significant technical barrier for further developing the pharmaceutical application of FDM printing<sup>14,17</sup>. Filaments not suitable for printing can be generally classified into the following three situations<sup>22,23</sup> (Fig. 1.1): 1) The brittle filaments can be broken by feeding gears (Fig. 1.1a); 2) The soft filaments cannot be pushed forward through the nozzle (Fig. 1.1b); 3) lacking enough stiffness, the surface of filaments can be scratched by feed gearings (Fig. 1.1c). Several methods have been utilized or developed to evaluate filament's feedability and printability, such as Repka-Zhang (R-Z) test<sup>17,24</sup>. Nasereddin et al. developed a technique that simulates the filament's feeding process through the printing head to screen the mechanical properties of HME filaments to predetermine their suitability for FDM. Zhang et al. established an R-Z method to

characterize the mechanical properties of HME filaments. Nevertheless, these current methods still cannot use a parameter to quantitatively predict the printability of a filament.

For the scope of this article, the term “printability of a filament” is used to describe the printing feasibility of one filament, and the term “process window of an FDM 3D printer” is used to describe the printability threshold of all filaments in one certain printer. This study aims to develop a quantitative method, the Xu-Repka-Zhan method, for filament printability evaluation. Three-point bend (3PB) test, stiffness test, and resistance test were employed to investigate the mechanical properties of filaments. One parameter, named “Toughness,” was utilized to represent filament printability quantitatively.

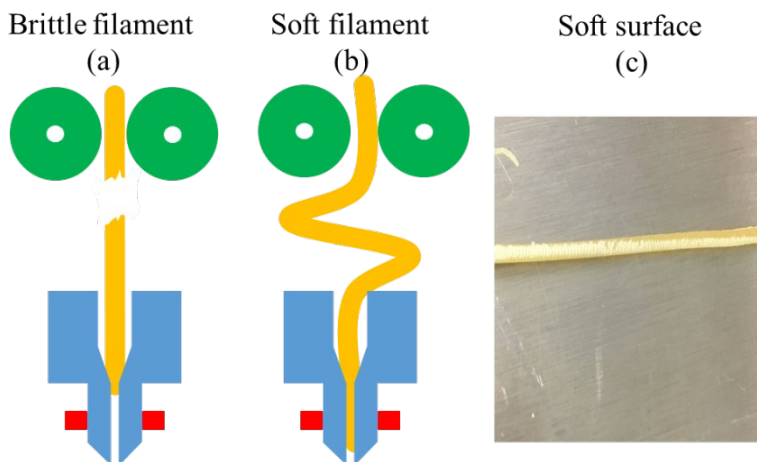


**Figure 1.1.** Illustration of different issues of filaments during printing. a) Brittle filament; b) Soft filament; c) Soft surface.

## 1.2. Materials and Methods

### 1.2.1. Materials

Indomethacin (98%) and polyethylene oxide (PEO; molecular weight = 100k-200k Da) were purchased from Acros Organics, Belgium. Affinisol HPMC HME 15LV & 100LV and Hypromellose Methocel K15M (HPMC K15M) were graciously donated by Colorcon, PA, USA. Polyethylene glycol 4000 (PEG 4K) was purchased from Alfa Aesar, MA. Kollidon VA 64 (PVP-

VA64) was purchased from BASF, NJ, USA. Klucel hydroxypropyl cellulose (HPC LF) and Aquasolve hydroxypropyl methyl cellulose acetate succinate (HPMC-AS HG) were from Ashland, NJ, USA. Polycaprolactone (PCL), poly (ethylene-co-vinyl acetate) (vinyl acetate 12 wt.%), and stearic acid were from Sigma-Aldrich. Parreck<sup>®</sup> M 200 (D-Mannitol) and Parreck<sup>®</sup> MXP EMPROVE<sup>®</sup> ESSENTIAL polyvinyl alcohol (PVA) were graciously provided from EMD Millipore, MA, USA. Eudragit RL PO was from Evonik, Germany. Polylactic acid (PLA) filament (1.75 mm) were purchased from Prusa (Prusa Research, Prague, Czech Republic). For dissolution medium preparation, potassium phosphate monobasic and sodium hydroxide were purchased from Jost Chemical (MO, USA) and J.T.Baker (PA, USA), respectively.

#### 1.2.2. Hot Melt Extrusion and Filament Fabrication

In-house filaments were produced by Hot melt extrusion (HME). Indomethacin and polymer excipients with various ratios were mixed using a Resodyn LabRAM II acoustic mixer at 60G for 1 min. The physical mixtures were then fed into the extruder at 3-5 g/min (depends on torque) using a magnetic feeder (Model: FTOC, Syntron) and then extruded (Process 11 Hygenic TSE, Thermo Fisher Scientific, Waltham, MA, USA) at a screw speed of 100 rpm with a standard screw configuration (Fig. 1.2). The melt extrusion was conducted using an 11-mm diameter co-rotating twin-screw with an L/D of approximately 40 and eight electrically heated zones. Pure HPMC and Indomethacin/HPMC formulations were extruded at 180 °C for all heating zones; all the other formulations were extruded at 160 °C for all heating zones. A 1.5-mm round-shaped die was used to extrude filaments for 3D printing. In addition, a conveyor belt was used to cool and straighten the filaments. Filaments with diameters of 1.6 mm ± 0.1 mm were collected and stored at ambient temperature in sealed clear plastic bags with gel desiccant for further characterization.

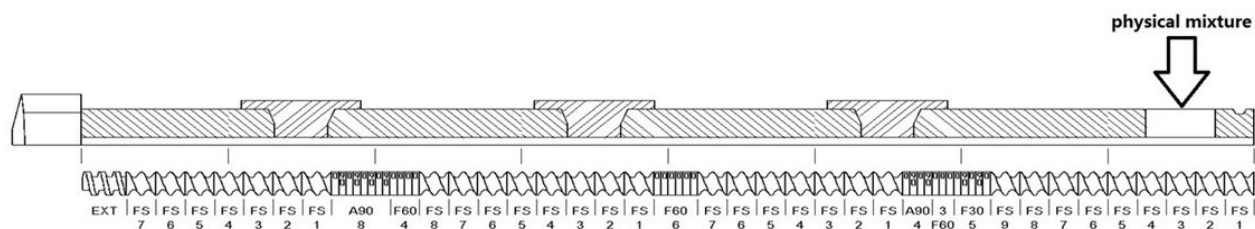


**Figure 1.2.** Standard hot melt extruder configuration.

### 1.2.3. Differential Scanning Calorimetry (DSC)

All samples were prepared with TA aluminum pans and lids (Tzero) with an average sample mass of 5-10 mg. Modulated DSC (mDSC) was conducted using a differential scanning calorimeter (Discovery DSC, TA Instruments, USA) at a heating rate of 3 °C/min. Modulated temperature change programmed with a sinusoidal oscillation of  $\pm 1$  °C/min. In all experiments, ultra-purified nitrogen was used as a purge gas with a 50 mL/min flow rate. Data were collected and analyzed using the Trios Data Analysis software (TA Instruments). All melting temperatures are reported as extrapolated onset unless otherwise noted.

### 1.2.4. Mechanical Characterization of Filaments

Three different texture analysis methods, using TA. XTPlus (Stable Micro Systems Ltd, Godalming, Surrey, UK) were utilized to measure the mechanical properties of filaments. Three-point bend (3PB) test was applied to measure the brittleness of filaments. Resistance test was used to measure the softness of filaments. Stiffness test was employed to measure the surface stiffness of filaments.

#### 1.2.4.1. 3PB Test

The Texture Analyzer was equipped with a three-point-bending rig with thin blades (3mm thickness). Filament was cut into 6cm lengths and placed on top of the three-point-bending holder. Trigger force was set to 5 g. The support span was set to 25 mm, and the test speed was set to 10

mm/s. 10 mm is the maximum distance below the supported filament. The maximum force and fracture distance were recorded by Texture Analyzer software. The area under the curve (AUC) and maximum stress were calculated using the Macro program in Texture Analyzer software. Ten homogenized filaments were characterized for each formulation. The illustration of 3PB is shown in Figure 1.3a.

Three anchors are inserted in the plot using the Macro program in the texture analysis software (Fig. 1.4a). Anchor 1 is set at the starting point of strain, anchor 2 is at the max strain, and anchor 3 is at the end of the test when stress approaches zero. The area under the curve between each two anchors is recorded. The AUC between anchor 1 and 2 was colored in red. The AUC between anchor 2 and 3 was colored in green. As shown in Figure 2a, the AUC between anchor 2 and 3 is not available for fractured filament due to the cracking of filament. The sum of red and green areas was named Brittleness in this study (Table 1.2).

#### 1.2.4.2. Resistance Test

The speed of resistance test was adapted from a previous study by Nasereddin et al. (2018). The Texture Analyzer was equipped with a cylinder rig. The filament was cut into 4cm lengths and place on top of the Texture Analyzer platform. Two 3D printed holders with a 2 mm hole at the center were attached to the probe and platform, respectively. The two loose ends of filaments were fixed inside the hole of the holder (Fig. 1.3b). Trigger force was set to 100 g, and 15% strain was used as press distance, speed is set to 1 mm/s. The maximum force and fracture distance were recorded by Texture Analyzer software. The area under curve (AUC) and maximum stress were calculated using the Macro program in Texture Analyzer software. Ten homogenized filaments were characterized for each formulation. The illustration of the resistance test was shown in Figure 1b.

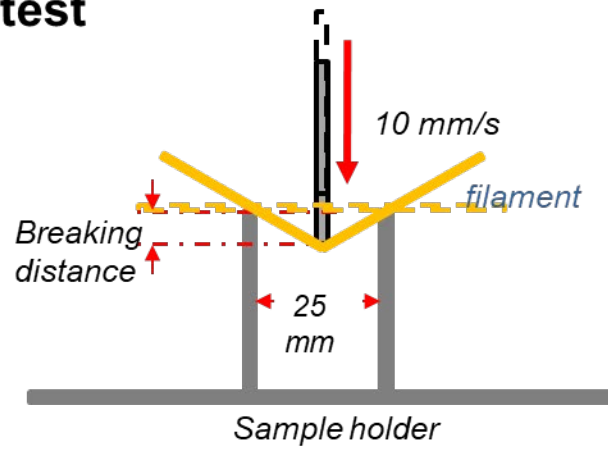
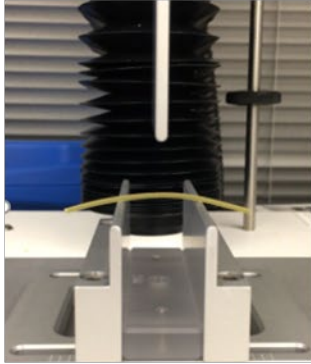
Like the 3PB test, three anchors are inserted in the plot using the Macro program in the texture analysis software (Fig. 1.4b). For the fractured filament, the AUC between anchor 2 and 3 is also missed. Resistance is named the sum of AUC between anchor 1 & 2 and anchor 2 & 3 in this study (Table 1.2).

#### 1.2.4.3. Stiffness Test

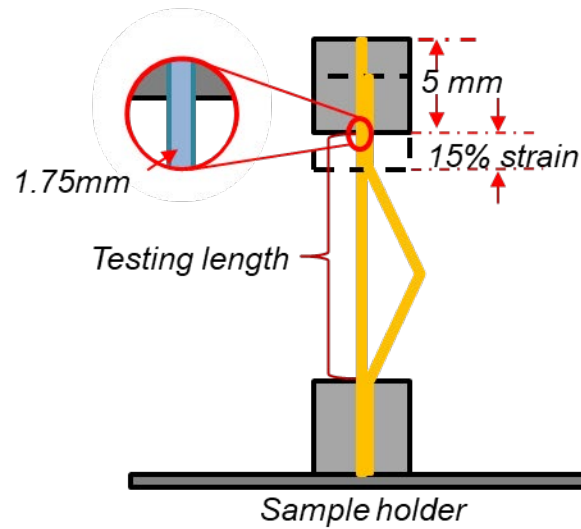
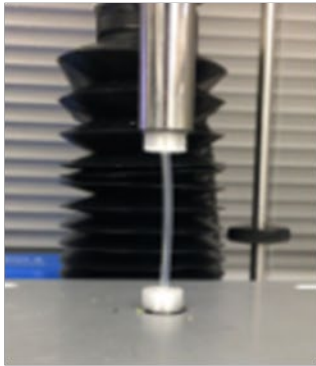
The Texture Analyzer was equipped with a three-point-bending rig with thin blades (3mm thickness). The filament was cut into 6 cm in length and placed on the Texture Analyzer platform. Trigger force was set to 50 g, and the blade was set to cut filament until 57% strain (~1 mm in the distance) at a speed of 2 mm/s. The maximum force and fracture distance were recorded by Texture Analyzer software. The AUC and maximum stress were calculated using the Macro program in Texture Analyzer software. Ten homogenized filaments were characterized for each formulation. The illustration of the stiffness test was shown in Figure 1.3c.

Similarly, there are three anchors in the plot of the stiffness test (Fig. 1.4c). The AUC between anchor 2 and 3 is missed for the fractured filament. The sum of AUC between anchor 1 & 2 and anchor 2 & 3 in this study is named Toughness (Table 1.2).

### a. Three-point bend test



### b. Resistance test



### c. Stiffness test

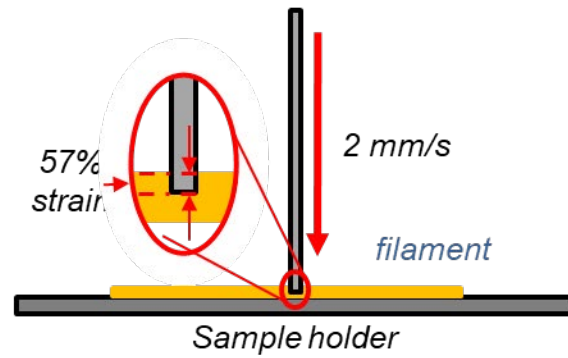
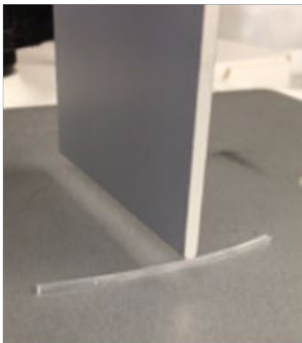
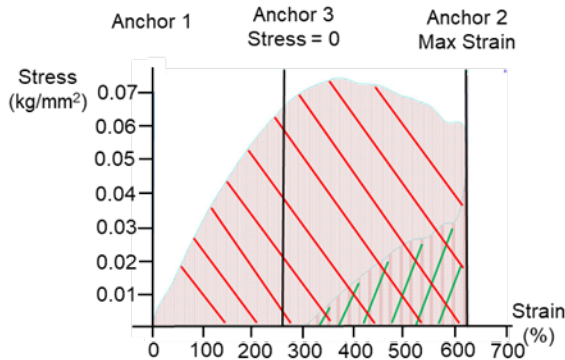


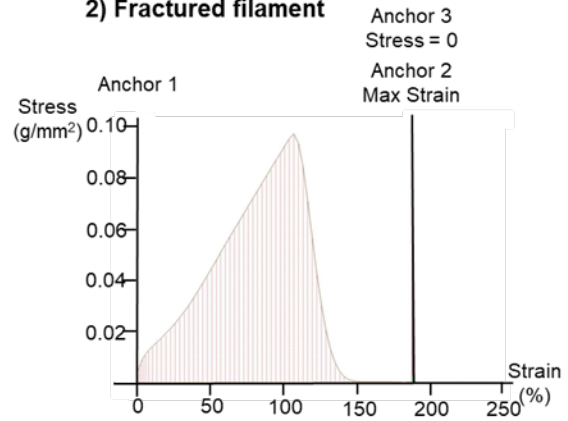
**Figure 1.3.** Texture analyzer setup for filament mechanical property test a) Illustration of three-point bend test b) Illustration of Resistance test. c) Illustration of stiffness test.

**a. Three-point bend test**

**1) Not fractured filament**

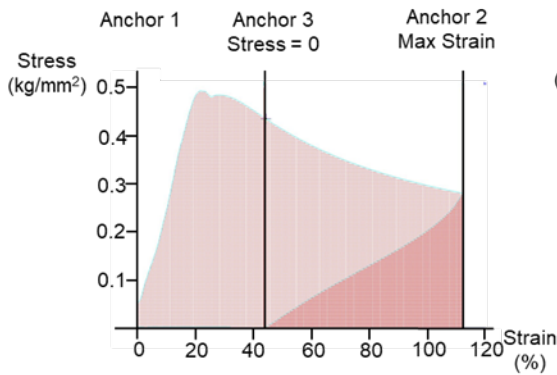


**2) Fractured filament**

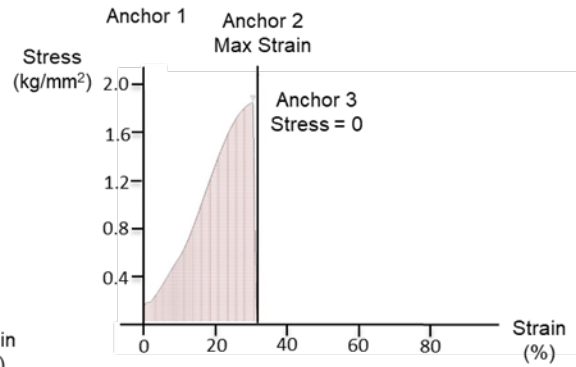


**b. Resistance test**

**1) Not fractured filament**

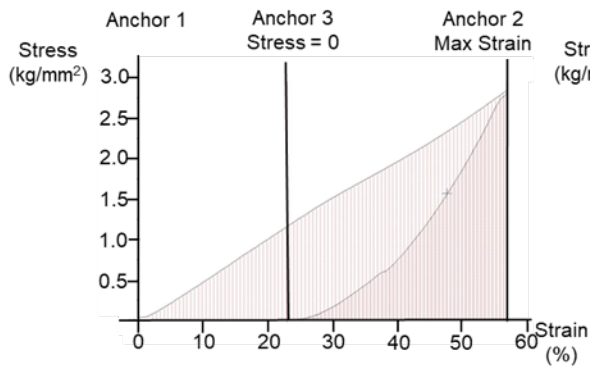


**2) Fractured filament**



**c. Stiffness test**

**1) Not fractured filament**



**2) Fractured filament**

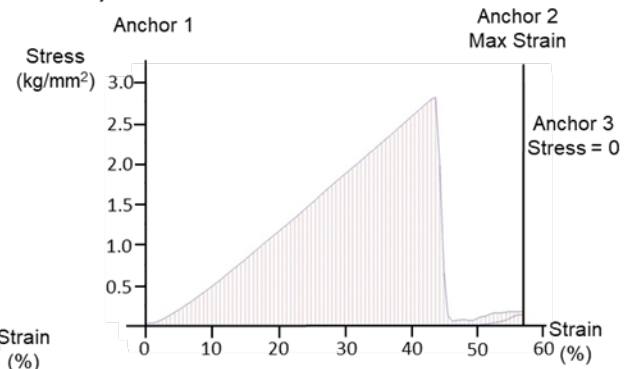


**Figure 1.4.** Texture analysis plots a) Three-point bend test b) Resistance test c) Stiffness test.



### 1.2.5. 3D Printer Setup and Printability Test

All filaments were tested in Prusa I3 MK3S 3D printer (Prusa Research, Prague, Czech Republic). The 3D printer is set-up as extrusion temperature 205-215 °C, bed temperature 40-60 °C, printing speed 50 mm/s, nozzle traveling speed 50 mm/s, layer height 0.10 mm. A cylinder shape tablet model, with 8 mm in diameter and 6 mm in height, was created using PrusaSlicer software. The infill structure of the tablet was set as 50% rectilinear infill without top and bottom cover layers. The filament is stated as “Yes” for Printability if it can be fed and printed into the model cylinder tablet at setup condition more than 3 times; Otherwise, the filament is labeled as “No” for Printability in Table 1.1.

All filaments were tested in Prusa I3 MK3S 3D printer (Prusa Research, Prague, Czech Republic). The 3D printer is set-up as: extrusion temperature 205–215 °C, bed temperature 40–60 °C, printing speed 50 mm/s, nozzle traveling speed 50 mm/s, layer height 0.10 mm. For model drug indomethacin, the degradation temperature is around 277.6 °C, and the TGA data showed that there was negligible weight change for indomethacin at 215 °C (Fig. 1.5). Therefore, a printing temperature around 205–215 °C was chosen for all filaments based on our internal data as well as the previous publications (Goyanes et al., 2015, 2017, 2016; Melocchi et al., 2016; Solanki et al., 2018; Zhang et al., 2017). A cylinder shape tablet model, with 8 mm in diameter and 6 mm in height, was created using PrusaSlicer software. The infill structure of the tablet was set as 50% rectilinear infill without top and bottom cover layers. The filament is stated as “Yes” for Printability if it can be fed and printed into the model cylinder tablet at setup condition more than 3 times; Otherwise, the filament is labeled as “No” for Printability in Table 1.1.

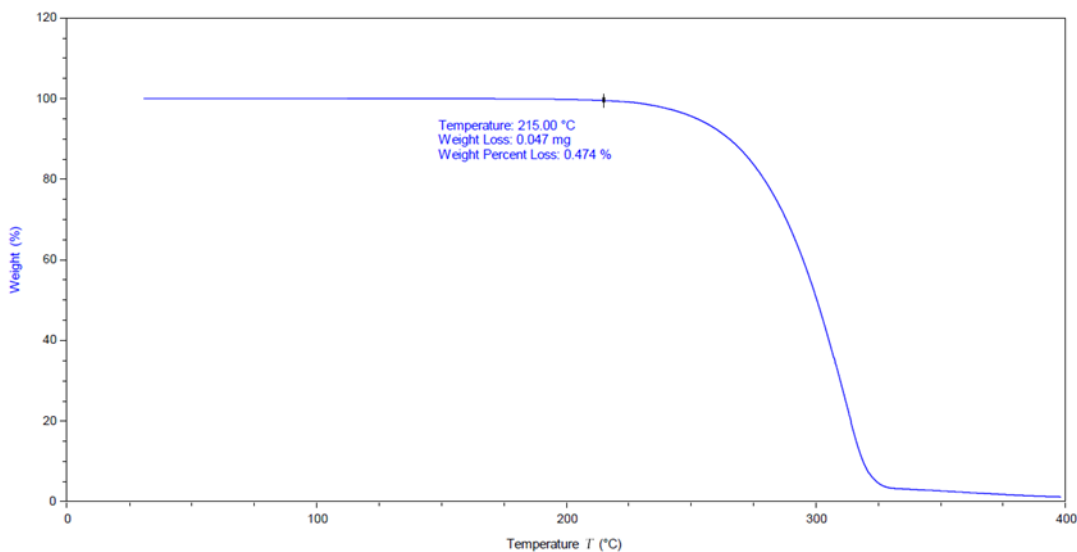


**Figure. 1.5.** Thermogravimetric Analysis of Indomethacin

#### 1.2.6. Oral Tablet Characterization

The appearance of representative 3D printed tablets was shown in Figure 1.9. A four decimal Mettler Toledo balance (model MS204S) was used to check tablet weight. Digital Caliper (manufacture) was utilized to measure the diameter and thickness of tablets. The hardness of the tablet was accessed by Tablet Harness Tester (Pharma Test, PTB 302). The average of three tablets was calculated for each formulation.

#### 1.2.7. Dissolution

The dissolution condition for testing of representative 3D printed tablets was derived from USP monograph for Indomethacin capsule. The dissolution medium was prepared with pH 7.2 phosphate buffer and water at 1:4 ratio. Experiments were conducted on apparatus I (basket) (Hanson Vision Elite 8 dissolution system) with online-UV detection (Pion R2D rainbow dynamic dissolution monitor system with 5mm pathlength probes). Each tablet was dissolved in 750 mL of degassed dissolution medium (Distek ezFill 4500) at 37 °C with the agitation speed at 100 rpm. The tablets were weighed, and the dissolution profile is normalized based on the actual API content

for each tablet. To minimize the excipient interference, second derivatives of UV absorbance of range 295-325 nm was selected to monitor the signal in the vessel. The calibration curves were built from 0-120% of the nominal concentration of 0.06 mg/mL, and the R2 of all the six channels are all above 0.999. The dissolution profile is shown in Figure 1.9.

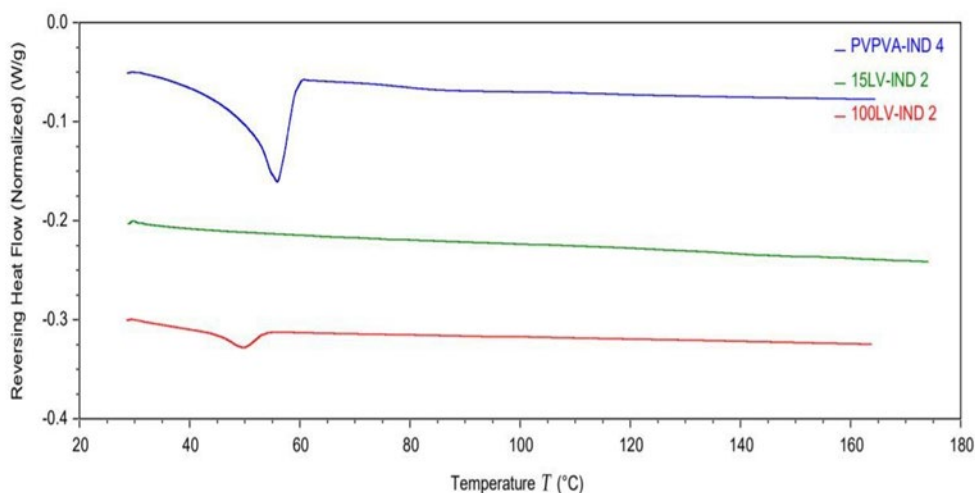
### **1.3. Results**

#### **1.3.1. Polymers Behavior in HME and Filament Printability Test in FDM 3D printing**

A model drug, indomethacin, was utilized in this study with a drug loading as 30% for method and process development. It is a small molecule drug with a melting point around 157 °C. Three different types of polymers, with various solubility, have been extruded with indomethacin, respectively, in order to evaluate the filament mechanical properties and investigate the release performance.

HPMC in three different grades, K15M, HME 15LV, and HME 100LV, was evaluated as a control release polymer in this study. HPMC K15M, with high molecular weight and melt viscosity, cannot be extruded alone at 180 °C due to high torque and pressure. Loaded with 30% indomethacin, Indo/HPMC K15M filament can be extruded at 180 °C, while indomethacin acts as a plasticizer during the HME process to reduce the torque and pressure. The diameter of filaments with the HPMC K15M matrix is barely influenced by the convey belt and is around 1.42-1.45 mm, which is very close to the diameter of the die (1.50 mm). Filaments with HPMC K15M, in general, were relatively brittle and hard to stick onto the printing bed during the FDM printing process. Adding plasticizers, such as PEO and HPC, greatly improved the stickiness and flexibility of filaments as previously shown in the literature<sup>22</sup>. HPMC HME 15LV and 100LV, developed especially for the HME process, have molecular weights as 90k and 180k, respectively. HPMC HME polymer has a lower melt viscosity enabling it to be processed by HME without plasticizers.

As shown in Table 1.1, HPMC HME can be extruded alone at 180 °C under medium torque (4-6.5 N\*m) and medium pressure (25-60 bar). The diameter of filaments with HPMC HME matrix can easily be controlled by the convey belt to around 1.7 mm due to its low melt viscosity. The surface of HPMC HME matrix filaments was relatively rough. DSC data showed all drug-loaded filaments



with HPMC HME matrix were amorphous (Figure 1.6). In the FDM printing process, all indomethacin-loaded HPMC HME filaments stuck onto the printing bed well even without a plasticizer. HPMC HME grade is preferred over K15M in FDM application, considering the ease of extrusion and filament printability.

**Figure 1.6.** Differential Thermal Analysis of Indomethacin filaments used in the tablet printing and dissolution experiments. The formulations of filaments are PVPVA-IND4, 15LV-IND2 and 100LV-IND2, respectively.

HPMC-AS HG was evaluated as delay release polymer in this study thanks to its pH sensitive properties. The extrusion torque and pressure of HPMC-AS HG alone are medium (9.1 N\*m, 52 bar) at 160 °C, while they were dropped dramatically by adding indomethacin or other plasticizers. The diameters of HPMC-AS HG matrix filaments with different plasticizers were significantly larger than the die diameter due to the “die swell” phenomenon, which depended on the viscoelastic properties of the polymers<sup>18</sup>.

For the immediate-release type of polymer, PVA, PVP VA64, Eudragit RL, and PEO were chosen in this study. All formulations using these polymers as matrices could be extruded with low torque and pressure (1.3-5.1 N\*m, 4-23 bar). However, none of them were printable with 30% indomethacin loading using Prusa I3 MK3S 3D printer. The most common issue is the brittleness of filaments. For instance, pure PVA filament made in-house or purchased from the supplier is printable, whereas 30% indomethacin-loaded PVA filament was fractured during printing. By adding sorbitol as the plasticizer, the mechanical property of Indo/PVA filament could be greatly improved, which is consistent with the observation in a recent publication. An immediate-release dosage was successfully developed with carvedilol and haloperidol<sup>12</sup>. However, with a high indomethacin loading of 30% in our study, PVA immediate-release filaments did not achieve enough mechanical property for FDM printing.

**Table 1.1.** Characterization and printability of in-house manufactured filaments

Label	API	Polymer	Plasticizer	Torque (N*m)	Pressure (bar)	Diameter(mm)	Printability
PLA-1	0% indomethacin	PLA-filament	N/A			1.75	Yes
PVA 1	0% indomethacin	PVA-filament	N/A			1.7	Yes
PVA2	0% indomethacin	100% PVA	N/A	9	53	1.6	Yes
PVA-IND 1	30% indomethacin	70% PVA	NA	6.1	24	1.5	No

K15M-IND	30%	70% HPMC	N/A	2.6	70	1.45	No
1	indomethacin	K15M					
K15M-IND	30%	60% HPMC	10% PEO	1.9	70	1.42	Yes
2	indomethacin	K15M					
K15M-IND	30%	60% HPMC	10%	2.2	27	1.44	No
3	indomethacin	K15M	PEG4k				
K15M-IND	30%	60% HPMC	10% HPC	2	64	1.42	Yes
4	indomethacin	K15M	LF				
K15M-IND	30%	60% HPMC	10%	1.3	75	1.45	Yes
5	indomethacin	K15M	stearic acid				
100LV-1	0%	100% HPMC	N/A	6	56	1.5	Yes
	indomethacin	HME 100LV					
100LV-2	0%	90% HPMC HME	10% PEO	6.3	57	1.7	Yes
	indomethacin	100LV					
100LV-IND	30%	60% HPMC HME	N/A	6	26	1.6	Yes
1	indomethacin	100LV					
100LV-IND	30%	60% HPMC HME	10% PEO	4.5	47	1.6	Yes
2	indomethacin	100LV					
100LV-IND	30%	60% HPMC HME	10% PCL	4	25	1.7	Yes
3	indomethacin	100LV					
ASHG 1	0%	100% HPMC-AS	N/A	9.1	52	1.7	Yes
	indomethacin	HG					

ASHG 2	0% indomethacin	95% HPMC-AS HG	5% HPC LF	7.9	56	1.75	Yes
ASHG 3	0% indomethacin	85% HPMC-AS HG	15% HPC LF	6.3	60	1.75	Yes
ASHG-IND 1	30% indomethacin	70% HPMC-AS HG	N/A	3.9	28	1.6	No
ASHG-IND 2	30% indomethacin	50% HPMC-AS HG	N/A	2.1	12	1.75	No
ASHG-IND 3	30% indomethacin	60% HPMC-AS HG	10% PEO	1.8	0	1.65	Yes
ASHG-IND 4	30% indomethacin	60% HPMC-AS HG	10% PEG4k	0.8	0	1.65	Yes
ASHG-IND 5	30% indomethacin	65% HPMC-AS HG	5% HPC LF	3.9	21	1.7	No
ASHG-IND 6	30% indomethacin	55% HPMC-AS HG	15% HPC LF	3.3	15	1.75	No
ASHG-IND 7	30% indomethacin	60% HPMC-AS HG	10% PCL	2.4	2	1.7	Yes
ASHG-IND 8	30% indomethacin	60% HPMC-AS HG	10% stearic acid	1.3	0	1.75	Yes
PVPVA 1	0% indomethacin	100% PVP VA64	N/A	5.1	23	1.75	No

PVPVA- IND 1	30% indomethacin	70% PVP VA64	N/A	2.1	5	1.75	No
PVPVA- IND 2	30% indomethacin	50% PVP VA64	N/A	1.3	4	1.75	No
PEO-IND 1	30% indomethacin	70% PEO	N/A	1.6	5	1.6	No
PCL-IND 1	30% indomethacin	70% PCL8k	N/A	2	5	1.7	No
EVA-IND 1	30% indomethacin	70% EVA	N/A	2	35	1.8	No
EUD-IND 1	30% indomethacin	70% Eudragit RL	N/A	2.1	0	1.75	No

### 1.3.2. Comparison of Three Texture Characterization Method and Identification of Toughness

In total, 41 different formulations of filaments were produced using HME. Among these 32 filaments, only 18 filaments were tested as printable using Prusa I3 MK3S 3D printer. To better evaluate the defects of filament, such as brittleness, softness and scratched surface, we simplify the characterization process and find the most critical mechanical properties to represent filament printability.

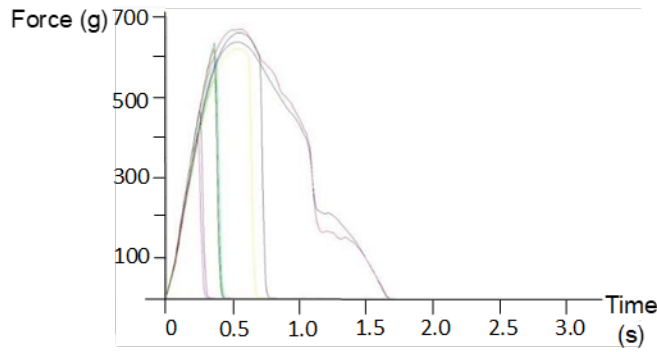
Repka-Zhang (R-Z) test is one of the most commonly used methods in the literature for the FDM filament characterization, which combined both the 3PB test and stiffness test<sup>24</sup>. In this study, we compared three texture analysis methods, 3PB test, resistance test and stiffness test, and the measurement data was a plot with Y-axis as Stress and X-axis as Strain (Fig. 1.4). Non-fractured flexible filament and fractured brittle filament showed distinguished plots all three tests (Fig. 1.4). Brittle filament broke at the peak stress before reaching the set strain value, while stress applied



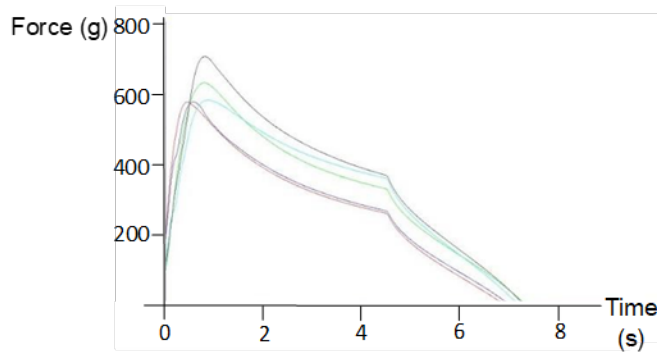
on flexible filament bounced back after the set strain value and went back to zero. A summary of brittleness, resistance and toughness were shown in Table 1.2. Compared to Brittleness and Resistance value measured by 3PB and resistance methods, respectively, Toughness valued by stiffness method has relatively low variation, which indicates good reproducibility of each measurement (Table 1.2, Fig. 1.7). In general, Indomethacin-loaded filaments exhibited lower Toughness, Brittleness and Resistance values compared to the pure polymer filaments. With a certain plasticizer, the mechanical property of the filament can be improved. For instance, by

adding 10% HPC LF and 10% Stearic acid, respectively, the Toughness, Brittleness and Resistance value of Indomethacin loaded HPMC K15M filaments are significantly enhanced (Table 1.2).

**a. 3PB test**



**b. Resistance test**



**c. Stiffness test**

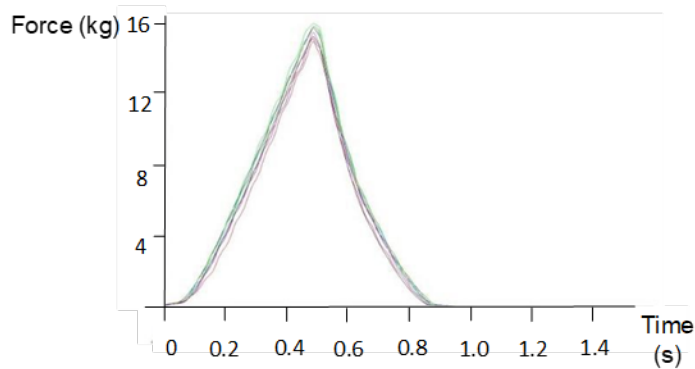


**Figure 1.7.** Representative measurements of filament in 3PB test (a, 10 measurements), Resistance test (b, 5 measurements) and Stiffness test (c, 10 measurements).

In Figure 1.8, the filaments type was arranged based on Toughness, Brittleness and Resistance values from high to low, while the red column indicated the non-printable filament using Prusa I3 MK3S FDM printer. In general, filaments with high Toughness, Brittleness or Resistance value can be printed, whereas filaments had low mechanical properties failed the printing test. Brittleness and Resistance plots were unable to differentiate the non-printable filaments by the value very well, there is a mixture of green (printable) and red (non-printable) column at the medium range of the figures. Interestingly, the Toughness plot, however, showed a good correlation with printability and we observed a distinguished boundary between printable and non-printable filaments. A threshold value as 80 g/mm2\*% was identified as the lowest Toughness requirement for Prusa I3 MK3S printing, therefore is defined as process window of this FDM printer. This threshold value is validated by an additional eight in-house made filaments, and for three filaments (15LV-IND1, 15LV-IND2 and PVPVA-IND4) have a Toughness value larger than 80 g/mm2\*%, can be printed by this FDM printer (Table 1.2).

**Table 1.2.** Toughness, resistance and brittleness value of in-house filaments using texture analysis methods.

Label	Toughness (kg/mm2*%)	C.V.	Resistance (kg/mm2*%)	C.V.	Brittleness St-Strain (kg/mm2*%)	C.V.
PLA-1	249.9	1.5	171.9	4.1	117.0	6.1
PVA 1	132.1	2.1	89.5	4.2	85.8	2.8
PVA2	211.2	10.5	62.1	18.1	12.9	9
PVA-IND 1	38.6	6.0	53.7	15.0	7.1	15.3
K15M-IND 1	60.2	1.5	19.3	21.4	2.3	12.2
K15M-IND 2	95.2	1.5	15.4	19.0	7.1	12
K15M-IND 3	46.7	7.2	8.2	22.5	1.7	14.3

K15M-IND 4	89.6	12.1	32.0	11.8	5.8	11.2
K15M-IND 5	145.6	2.2	21.7	9.2	6.3	15.3
100LV-1	119.9	11.0	90.5	3.7	54.8	3.9
100LV-2	149.1	3.8	55.6	6.3	51.4	2.6
100LV-IND 1	161.4	2.7	112.0	6.1	24.0	25.7
100LV-IND 2	137.0	3.2	51.5	13.1	53.2	9.1
100LV-IND 3	164.3	4.7	46.8	7.2	44.5	7.7
ASHG 1	155.6	3.2	121.7	21.2	90.3	14.3
ASHG 2	181.4	2.3	123.0	26.1	142.6	25.7
ASHG 3	171.3	1.2	147.4	7.3	138.5	8.7
ASHG-IND 1	60.8	19.9	35.9	10.5	4.5	13.9
ASHG-IND 2	25.6	9.5	29.9	21.6	3.2	7.1
ASHG-IND 3	153.2	4.3	29.0	11.4	28.8	65
ASHG-IND 4	142.2	3.6	55.6	15.2	8.3	33.7
ASHG-IND 5	66.0	6.4	30.7	12.2	4.5	10.5
ASHG-IND 6	40.5	16.7	32.7	8.3	4.5	24.5
ASHG-IND 7	80.3	15.0	29.7	21.1	6.3	17.9
ASHG-IND 8	141.4	3.8	53.4	63.2	8.5	20.4
PVPVA 1	47.4	6.6	11.6	8.6	3.4	23.7
PVPVA-IND 1	31.6	7.2	23.9	9.0	2.4	5.4
PVPVA-IND 2	15.1	5.5	13.6	33.4	1.8	18.4
PEO-IND 1	49.8	6.5	23.2	17.2	16.9	21.9
PCL-IND 1	53.3	3.6	15.7	15.0	51.7	19.7
EVA-IND 1	33.3	1.3	12.9	13.3	6.3	26.7

EUD-IND 1	18.4	11.7	15.9	18.9	2.4	5.6
-----------	------	------	------	------	-----	-----

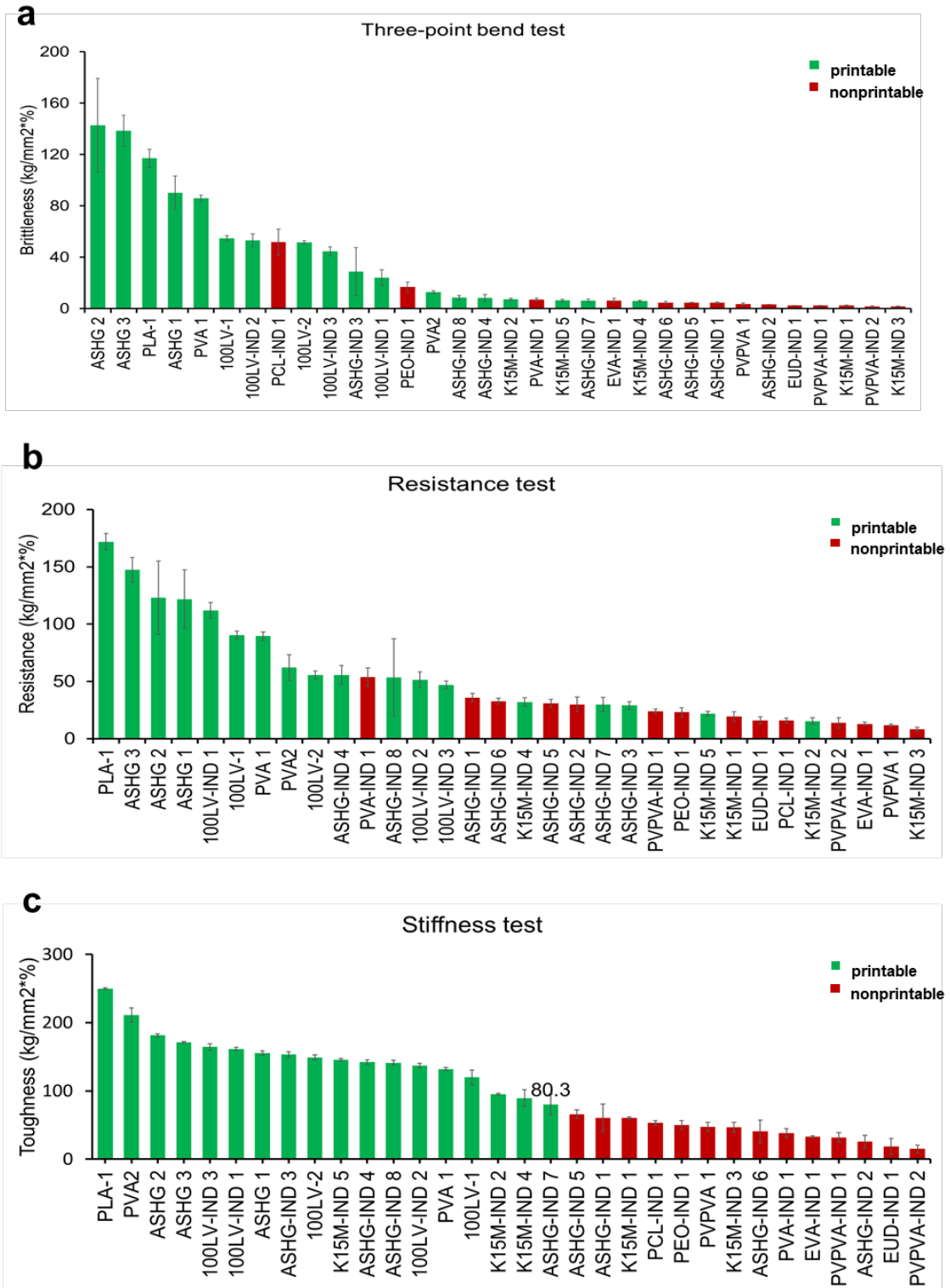
### 1.3.3. Characterization and Dissolution of 3D Printed Tablets Using Filaments with Different Toughness Values

In order to demonstrate the printability of filament with various toughness values, three filaments were chosen for model tablet printing (Figure 1.9). Indomethacin/PVP-VA/PEO filament shows the lowest toughness value among these three filaments as 89.1 g/mm<sup>2</sup>%, which is close to the printing threshold of 80 g/mm<sup>2</sup>% of Prusa I3 MK3S 3D printer. Indomethacin/HPMC-HME-100LV/PEO exhibits the highest value as 137 g/mm<sup>2</sup>% while Indomethacin/HPMC-HME-15LV/PEG shows an intermediate toughness as 115 g/mm<sup>2</sup>%. Indomethacin was in the amorphous form in all three filaments (Figure 1.6).

The printing of tablets was conducted at an optimized temperature for both hot end and printing bed. All three filaments were successfully printed into a rectilinear infill structure model tablet, shown in Figure 1.9, without apparent flaws. And with 0.10 mm resolution, the tablet printing has excellent reproducibility, and the weight variation between different printing batches was minimum. PVP-VA matrix tablet shows a brighter yellow color appearance and relatively low hardness as 10.50 kp, which is consistent with the lower toughness property of its filament. HPMC-15LV and HPMC-100LV matrix tablets achieved a similar hardness value as 24.37 kp, and all three types of tablets are hard enough to handle and perform the characterization.

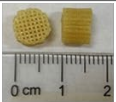
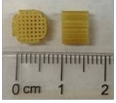
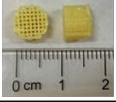
The dissolution profile of three types of tablets is shown in Figure 1.9. HPMC is commonly used in extended-release formulation<sup>25,26</sup>. Two HPMC matrix tablets exhibited extended-release profiles as expected. With relatively lower molecular weight, HPMC-15LV tablet reached the 80% drug release after 10 hours, while it requires 18h for higher molecular weight HPMC-100LV tablet obtain the same release percentage. Surprisingly, as a soluble polymer, the PVP-VA matrix tablet

shows a slower dissolution profile and achieved 80% drug release after 7 hours. It might be due to the high percentage of PEO composition, which slower the disintegration of tablet and the diffusion of Indomethacin within the matrix.



**Figure 1.8.** Correlation between the filament printability and the toughness, brittleness, resistance values measured by a) three-bend test, b) resistance test, c) stiffness test, respectively.

### Characterization of 3D printed tablets using filaments with different toughness values

Label	Composition	Filament Toughness (g/mm <sup>2</sup> *)	Appearance	Diameter (mm)	Thickness (mm)	Weight (mg)	Hardness (kP)
PVP-VA	Indomethacin 30% PVP-VA64 40% PEO10K 30%	89.1		7.89±0.03	5.79±0.13	149.97±2.20	10.50±0.71
HPMC-15lv	Indomethacin 30% HPMC-15lv 60% PEG4K 10%	115.0		7.76±0.03	5.76±0.03	164.60±0.32	24.37±2.69
HPMC-100lv	Indomethacin 30% HPMC-100lv 60% PEO10K 10%	137.0		7.84±0.01	5.78±0.03	164.27±0.73	24.37±1.50

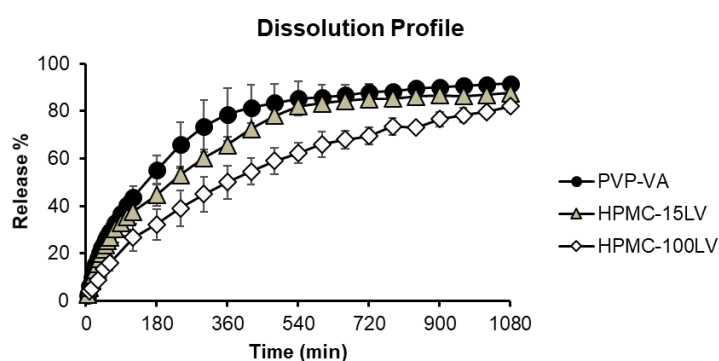


**Figure 1.9.** Characterization and dissolution of 3D printed tablets using filaments with different toughness values (n=3). Black round: Tablet contained 30% Indomethacin, 40% PVP-VA64 and 30% PEO10K; Grey triangle: Tablet contained 30% Indomethacin, 60% HPMC-15lv and 10% PEG4K; White diamond: Tablet contained 30% Indomethacin, 60% HPMC-100lv and 10% PEO10K.

#### 1.4. Discussion

Compared to traditional pharmaceutical manufacturing, 3DP has greater flexibility and cost benefits since it could significantly reduce the footprint and waste. It could also challenge the current supply chain distribution, quality, and regulatory system, considering an extreme case that the drug product filament as an intermediate product to be distributed worldwide while the final product is printed in the pharmacies. The lack of conventional quantitative characterization



methods for filament printability has been recognized as a critical barrier to the FDM application. In this research, we compared three texture analysis methods, and a parameter “Toughness” has been selected to characterize the printability of FDM filament quantitatively. At the stage of drug-loaded filament development, this method can be used as an indicator for filament feasibility and optimization. More importantly, for analytical characterization and quality control point of view, this method provides a quantitative way to describe the filament product specification during manufacturing.

In this study, three different methods were utilized to measure the mechanical properties of filaments. Among these three methods, the stiffness test has more significant advantages and can provide a more accurate and reliable result. 1) Easy operation. Compared to the other two methods, the stiffness method requires only a blade probe without specific holders or platforms. 2) Less material. For each test of 3PB and resistance test, 6 cm or 4 cm length filament was consumed, respectively, while stiffness test needs only around 1 cm length. Considering 10 sample measurements to achieve a more statistical result, the amount of material required for these tests will be a burden, especially for research stage work with limited active pharmaceutical ingredients. 3) Less deviation. As shown in Table 1.2, the deviations of the 3PB test and resistance were much higher than the stiffness test due to the lower reproducibility of each test.

In the previous studies, the R-Z test and Texture Analysis Screening test were applied to evaluate the printability of filament<sup>17,24</sup>. However, the parameters used in those studies, such as fracture point, yield strength, young’s modulus, maximum stress and breaking distance, cannot represent the printability with high accuracy alone. The 3PB test plot and stiffness plot of two filaments were shown in Figure 1.10a and 1.10b, respectively. For the 3PB test, in Figure 1.10a, non-printable filament (INDO-PCL 3-7) is too soft to print, although it exhibits a higher max force

and breaking distance than printable filament (INDO-HPMCAS-PCL 3-6-1). When using the stiffness test, max force is still not the best way to describe filament printability. As shown in Figure 1.10b and in the table, in practice, F2 is printable while F1 is too brittle to print. Compared to the maximum stress of these two filaments for Stiffness test, F1 exhibits a higher value than F2, although it breaks at the maximum stress. On the contrary, Toughness result from stiffness test shows a more reasonable comparison for the filaments (Fig. 1.10). Therefore, Toughness calculated using AUC provides a more comprehensive way to characterize the mechanical property of filament.

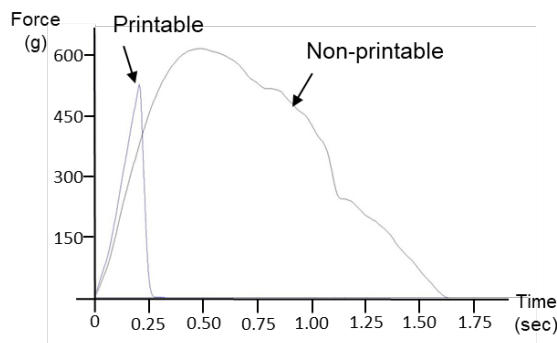
In application, this toughness value could also provide quantitative evidence to guide the selection and improvement during filament development. For example, in Figure 1.11, Indomethacin/HPMC-K15M filaments with various plasticizers were characterized using this method. It clearly shows that with the plasticizer such as stearic acid, PEO and HPC-LF could improve the mechanical property of the filament and stearic acid has more advanced improvement compared to the other two. Meanwhile, PEG8K worsens the printability with a lower toughness

value.

**Comparison of filament printability evaluation using max force and toughness values.**

Label	Formulation	Max Force (g)	Toughness (g/mm <sup>2</sup> *%)	Printability
F1	Indomethacin 30% HPMC-AS HG 65% HPC LF 5%	17830	66	No
F2	Indomethacin 30% HPMC K15M 60% Stearic acid 10%	14460	146	Yes

**a) 3PB test plot of a fractured filament**



**b) Stiffness test plot of fractured and non-fractured filaments**

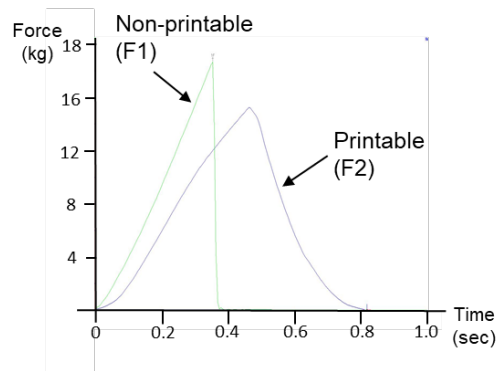


**Figure 1.10.** Comparison of filament printability evaluation using max force and toughness values in 3PB test and Stiffness test, respectively.

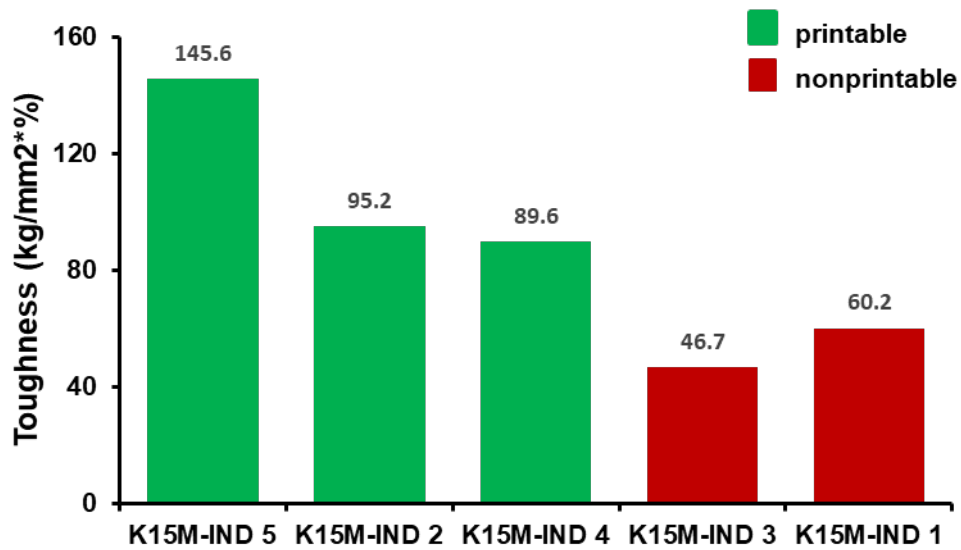
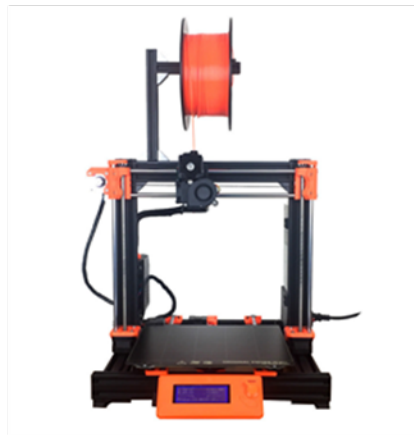


**Figure 1.11.** The Printability and Toughness evaluation of Indomethacin/HPMC K15M filament with various plasticizers.

In addition, this toughness test provides an alternative way to predict and evaluate the filament without testing it in a real 3D printer, which could not only save materials, time and cost, but also greatly improve the efficiency and ease to transfer the 3D printing process from one brand of printer to the others. By detecting and collecting this numeric value for various filaments, a database of filament printability and 3D process window can be built to the FDM 3D printing knowledge base as a reference for the improvement of both filament and 3D printer development. Filaments with certain toughness values could be grouped as a calibration kit to detect the process window of a new 3D printer to predict the drug product filament printability, which can greatly accelerate the development process during tech transfer.

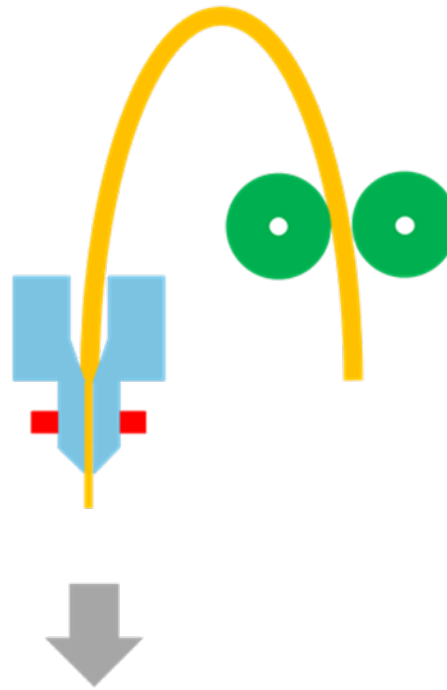
One thing that needs to be pointed out is that we mainly focused on the direct extrusion type of FDM in this study. The major difference between direct extrusion FDM (Fig. 1.12a) and Bowden extrusion FDM (Fig. 1.12b) integrates the feeding system and hot end<sup>27</sup>. The feeding system of the direct extrusion printer is integrated with the hot end and directly pushes the filament into the nozzle. On the contrary, the feeding system of the Bowden extrusion printer mounted on the frame, the filament is pulled through a long PTFE Bowden tube into the moving hot end to print. In general, the direct extrusion has fewer requirements to the filament, especially for high drug-load filament, than Bowden extrusion. Since Bowden extrusion FDM might have different requirements on filament flexibility and stiffness due to the feeding tubes, the parameters obtained in this study using direct extrusion might not be entirely applicable for Bowden extrusion type. Additional work will be needed to expand the application of this method.

**a) Direct Extrusion**



**Prusa i3 MK3S**

**b) Bowden extrusion**



**Ultimaker 3s**

**Figure 1.12.** Two types of FDM 3D printers and commercial 3D printer examples. a) Direct extrusion; b) Bowden extrusion.

## **1.5. Conclusion**

The revolution of 3D printing technology brings benefits and challenges to the pharmaceutical industry. In this study, we compared three texture analysis methods and a parameter “toughness” has been selected to quantitatively characterize the printability of FDM filament. The correlation of filament mechanical properties and the FDM 3D printing process was investigated. At the stage of drug-loaded filament development, this method can be used as an indicator for filament feasibility and optimization. More importantly, from an analytical characterization and quality control point of view, it provides a quantitative way to describe the filament product specification during manufacturing.

## CHAPTER II

### INVESTIGATION OF DIFFERENT MATRIX TABLETS' DRUG RELEASE PROFILES WITH VARIOUS STRUCTURES AND WATERPROOF COVERS VIA FUSED DEPOSITION MODELING

#### 2.1. Introduction

The development of new drug molecules is time-consuming and expensive. The safety efficacy ratio of “old” drugs has been tried to improve by using different methods such as therapeutic drug monitoring, individualizing drug therapy and dose titration. Delivering drugs at targeted delivery, controlled rate, and slow delivery are other attractive approaches that have been heavily investigated<sup>1</sup>. Drug delivery systems (DDSs) are the method or processes of administering pharmaceutical compounds to achieve therapeutic effects in humans or animals. The aim of DDSs is to ensure optimal distribution and absorption of drugs and improve efficacy and safety by controlling the speed, time and target of drug release in the body<sup>28</sup>. Effective DDSs approaches include controlled-release agents, where the drug is released at a controlled rate over a period of time, and targeted delivery, where the drug is only effective in a targeted area of the body, such as cancerous tissue<sup>2,29</sup>. Controlled release technologies can be broadly divided into liposomes<sup>30</sup>, electromechanical<sup>31</sup> and polymer types<sup>32</sup>. Controlled delivery using liposomes has been studied extensively, but in vivo instability and reticuloendothelial system embedding are two major obstacles to be overcome<sup>33</sup>. The use of pumping devices to control drug release is the most direct and complex method. However, osmotic pump systems are much more expensive and can cause dose dumping if the membrane ruptured<sup>34</sup>. Polymer controlled release systems use biodegradable, non-biodegradable and soluble polymers as drug carriers, which can be delivered through the skin,

parenterally, implantable, orally and by insertion<sup>35</sup>. Currently, polymeric oral controlled release technologies are considered to be immediately applicable and economical for drug development, reducing the inconvenience caused by the frequent administration of conventional tablets and improving the quality of life of patients<sup>36</sup>.

In addition, the increased use of additive manufacturing(also known as 3D printing technology) provides an effective solution for complex patient-focus production of oral-controlled DDSs<sup>37</sup>. It is widely acknowledged that three-dimensional (3D) printing can disrupt and change the pharmaceutical industry's production model by enabling on-demand customization of personalized medicine<sup>38</sup>. The dose, size, shape, color, taste and release profile can be personalized. At all stages of drug development, from preclinical studies and the first-in-human (FIH) clinical trials to on-demand manufacturing in hospitals and pharmacies, 3D printing could revolutionize the way oral formulations are produced. The launch of Spritam<sup>®</sup>(Aprecia Pharmaceuticals LLC) demonstrates that 3D printing can also be used for the commercial production of oro-dispersible tablets<sup>6</sup>.

In 3D printing, digital models are created by using computer-aided design (CAD) software and objects are produced by depositing materials layer-by-layer. A wide range of advanced formulations has been fabricated by 3D printing, including personalized oral dosage forms with innovative structures<sup>39-41</sup>, oral disintegrating tablets<sup>42</sup> and drug combinations<sup>43-45</sup>, capsule devices<sup>46-48</sup> and medical devices<sup>49-52</sup>. These are challenging to traditional manufacturing methods. 3D printing has also been combined with microfabrication to produce personalized tablets with adjustable release profiles<sup>53,54</sup>. Fused deposition modeling (FDM) is one of the most commonly used 3D printing techniques in pharmaceutical research. FDM requires filament made of the



thermoplastic polymer as material, and the drug can be added by impregnation or hot-melt extrusion (HME)<sup>55-57</sup>.

This study aims to investigate the relationship between tablets' drug release profiles and different geometries and waterproof covers. Two different types of FDA-approved biopolymers, hydroxypropyl methylcellulose (HPMC) HME 15lv and Polyvinyl alcohol (PVA), were selected as excipients to deliver acetaminophen (APAP) due to their different release mechanism and release rate<sup>58,59</sup>. The impact of different geometries and waterproof covers on the *in vitro* drug release profiles were also investigated.

## **2.2. Materials and Methods**

### **2.2.1. Materials**

As a model API, Acetaminophen (APAP; Spectrum Chemical, New Brunswick, NJ, USA) was selected. APAP is crystalline and is considered a borderline compound between class I (high permeability, high solubility) and class III (low permeability, high solubility) in the Biopharmaceutics Classification System (BCS), with a melting point of 168-172 °C<sup>60</sup>. Affinisol<sup>®</sup> HPMC HME 15LV was graciously donated by Colorcon, PA, USA. Parteck<sup>®</sup> MXP (Polyvinyl alcohol) (PVA) was purchased from Millipore Corporation (Billerica, MA, USA). Mannitol powder was purchased from VWR Chemicals (Fountain Parkway, Solon, Ohio, USA). Polylactic acid (PLA) filament (2.85 mm) was purchased from LulzBot (Fargo, North Dakota, USA). For dissolution medium preparation, potassium phosphate monobasic and sodium hydroxide were purchased from Jost Chemical (MO, USA) and J.T.Baker, PA, USA, respectively.

### **2.2.2. Formulation**

Two different formulations were tried in this study (Table 2.1). To get the physical mixture, raw materials were mixed on a Maxiblend<sup>™</sup> (GlobePharma, New Brunswick, NJ, USA) at 25 rpm

for 30 min, after filtration through a US #30 mesh screen to remove any aggregates that may have formed.

**Table 2.1.** Operation parameters for the two different formulations during HME process.

Formulations	API (w/w) %	Polymer (w/w) %	Plasticizer (w/w) %	T (°C)	Torque (N*m)	Pressure (bar)
F1	20% APAP	80% HPMC	N/A	160	6.5	40
F2	20% APAP	70% PVA	10% mannitol	150	6.2	34

### 2.2.3. Hot Melt Extrusion and Filament Fabrication

Filaments were produced by the HME process. The physical mixture was then fed into the extruder and then extruded (Process 11 Hygenic TSE, Thermo Fisher Scientific, Waltham, MA, USA) at a screw speed of 50 rpm with a standard screw configuration. The melt extrusion was conducted using an 11-mm diameter co-rotating twin-screw with an L/D of approximately 40 and eight electrically heated zones. A 2.5 mm round-shape die was used to extrude filaments for 3D printing. A conveyor belt was used to adjust the diameter of filaments (2.6-2.85 mm) and straighten the filaments for feeding into the 3D printer.

### 2.2.4. Differential Scanning Calorimetry (DSC)

The drug crystallinity and characterize drug miscibility in the extrudates were studied by a differential scanning calorimeter (Discovery DSC, TA Instruments, USA). Samples (5-10 mg) were hermetically sealed in an aluminum pan and heated from 40 to 200 °C at a rate of 10 °C/min. Ultra-purified nitrogen was used as the purge gas at 50 mL/min flow rate in all DSC experiments. Data were collected and analyzed using the Trios Data Analysis software (TA Instruments). All melting temperatures are reported as extrapolated onset unless otherwise noted.

### 2.2.5. Thermogravimetric analysis (TGA)

During HME processing, a PerkinElmer Pyris 1 TGA calorimeter was used to determine the thermal stability of APAP and the polymers. The samples were placed in an open aluminum

pan and heated from 30 to 500 °C at a rate of 20 °C/min. Ultra-purified nitrogen was used as the purge gas at 25 mL/min flow rate. Data were collected and analyzed using Pyris software, and percentage mass loss and/or onset temperatures were calculated.

#### 2.2.6. Mechanical characterization of filaments

Three different texture analysis methods, using TA. XTPlus (Stable Micro Systems Ltd, Godalming, Surrey, UK) were employed to measure the mechanical properties of filaments. Three-point bend (3PB) test was applied to measure the brittleness of filaments. Resistance test was used to measure the softness of filaments. Stiffness test was employed to measure the surface stiffness of filaments<sup>61</sup>.

#### 2.2.7. Design of 3D geometry models

The models of all tablets were designed using Fusion 360 (Autodesk, Mill Valley, CA, USA), sliced using Ultimaker Cura software (version 4.10; Ultimaker, Geldermalsen, The Netherlands). The 3D models for the core (yellow part) and the cover (grey part) is illustrated in Figure 2.1. The first 3D model was a Cylinder with a 10 mm diameter and 3.2 mm thickness in the first line. The second 3D model was a Torus structure with 10 mm external diameter, 5 mm internal diameter and 3.2 mm thickness. The third 3D model was called Semicircle (Semi). Compared Semi to Torus, the only difference was the hollow middle part was divided into two halves and equally placed. The fourth 3D model was called Quadrant (Quad). The hollow middle part was divided into four Quads and placed equally. The 3D structures of covers were shown in the second line (Figure 2.1). The top and bottom thickness of covers were 1 mm, four rectangular solids with 1 mm length and width and 3.2 mm height were used to connect the top and bottom parts. The internal and external diameters of the top and bottom parts were the same as corresponding structures (cylinder, torus, Semi and Quad). Then new 3D designs models of each structure were

obtained by combinations of cover and core. The reason for designing the torus model is that if the thickness is constant and the erosion speed in the outer circle and inner circle is the same, then the surface area (SA) will be constant during the dissolution test. And the SA of Semi and the Quad will increase during the dissolution test. If SA of tablets can be controlled during dissolution, then drug release curve can be manipulated to some extent. In fact, the thickness of tablets will decrease due to erosion by the dissolution medium. So, the second part is the cover made by PLA. PLA is a waterproof material. The cover of PLA can prevent dissolution medium penetrates dosages from top and bot. And HPMC will swell during the dissolution test, and the pillars can lock the body of dosages so that the thickness will not increase due to swelling. So the thickness will be constant in theory. The SA in contact with the medium, volume (V) and SA/V ratio of each tablet were shown in Table 2.2.

**Table 2.2.** Geometric parameter of each tablet.

Geometries	Surface area (mm <sup>2</sup> )	Volume (mm <sup>3</sup> )	SA/V ratio (m <sup>-1</sup> )
Cylinder	257.6	251.3	1.03
Torus	268.6	188.5	1.42
Semi	300.6	188.5	1.59
Quad	332.6	188.5	1.76
Cylinder wC	100.5	238.5	0.42
Torus wC	150.8	175.7	0.86
Semi wC	182.8	175.7	1.04
Quad wC	214.8	175.7	1.22

The 3D models were then exported as stereolithography (.STL) files into 3D printer software (Ultimaker Cura software v. 4.10; Ultimaker, Geldermalsen, The Netherlands). The.STL format contained only the object surface data, and all the other parameters were defined from Cura software to obtain tablets with the best resolution.

### 2.2.8. 3D printing

Tablets were fabricated from the extruded filaments (cover: PLA filament, core: drug-loaded Filaments) using an Ultimaker 3S printer (Ultimaker, Geldermalsen, The Netherlands) with two extruders, which had two 0.4 mm nozzles. The parameters of the printing process were shown in Table 2.3.

**Table 2.3.** The parameters of 3D printing process.

Extruders	Extruder 1	Extruder 2	
Filaments	PLA	F1	F2
Printing part	Cover	Core	Core
Layer height (mm)	0.1	0.1	0.1
Shell thickness (mm)	0.4	0.4	0.4
Infill pattern and density	Lines, 100%	Lines, 100%	Lines, 100%
Print speed, Pattern speed (mm/s)	70, 70	40, 18	40, 18
Printing temperature (°C)	200	190	180
Building plate temperature (°C)	60	60	60

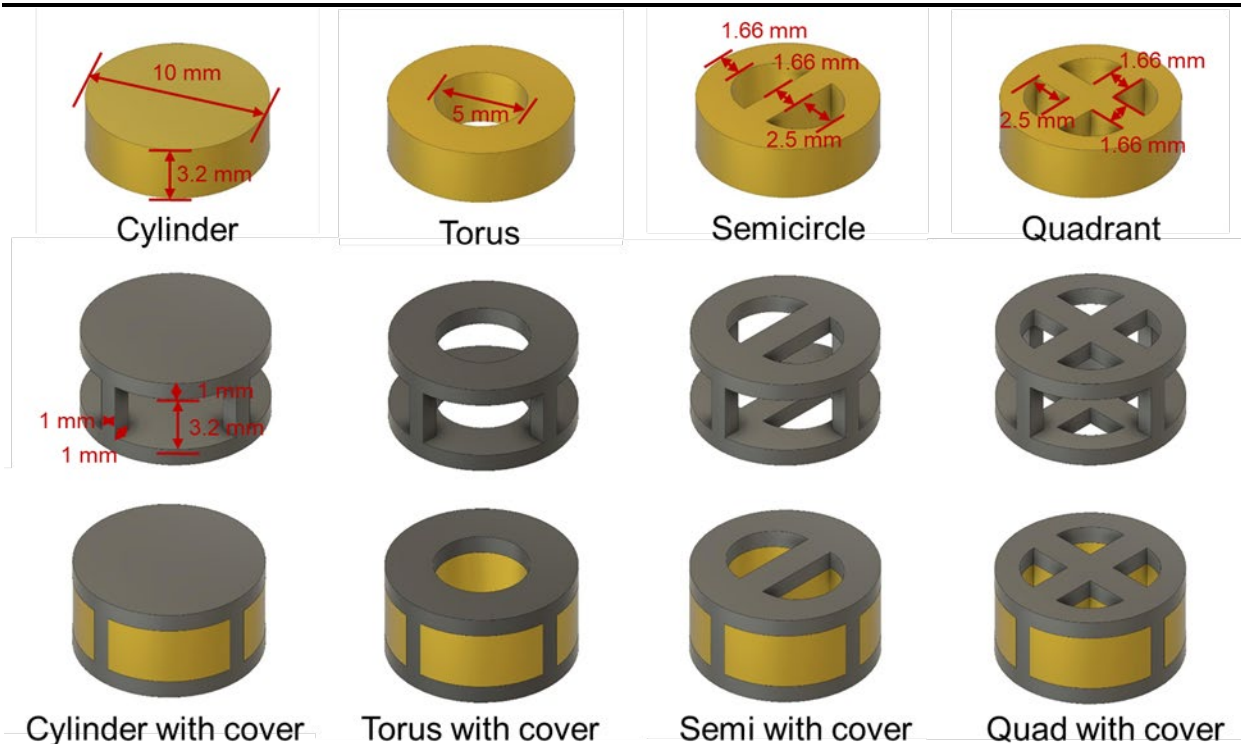


**Figure 2.1.** The 3D geometry design models of tablets.

## 2.2.9. Tablet characterization

### 2.2.9.1. Assessment of tablet morphology

A VWR1 digital caliper (VWR1, PA, U.S.) was used to determine the tablets' diameters and thicknesses. An iPhone 12 Pro Max was used to take images of tablets (Apple, Cupertino, CA). Cross-sectional images of filaments were taken using scanning electronic microscopy (SEM).

### 2.2.9.2. Determination of tablet strength

A standard tablet hardness tester (VK200; Agilent Technologies, Santa Clara, CA, USA) with a maximum force of 35 kp was used to measure tablet hardness. Six tablets from each group of tablets were tested.

### 2.2.10. *In vitro* drug release study

Drug release from different 3D geometries tablets was determined using a United States Pharmacopeia (USP) dissolution apparatus II (Hanson SR8-plus™; Hanson Research, Chatsworth, CA, USA). Dissolution tests were conducted as per US Pharmacopeia standards using Simulated Intestinal FluidTS (without pancreatin, pH 6.8), which is representative of the small intestinal fluid of humans. Each experiment was carried out in triplicate using 900 mL of dissolution medium at  $37 \pm 0.5$  °C for 24 h. The paddle speed was set at 50 rpm. Sinkers were used to keep the tablets submerged in the dissolution vessel. HPLC (Waters Corp, Milford, MA, USA) determined the amount of released APAP at 243 nm and analyzed using Empower software (version 2, Waters Corp).

### 2.2.11. Mathematical description and release models

The mean dissolution time (MDT) is used as a characteristic value that describe the drug release rate from the dosage form and the retarding efficiency of the polymer and was calculated

according to Equation (1)<sup>62-64</sup>. It is expressed in units of time a higher value of MDT indicates a higher drug retaining ability of the polymer and vice-versa.

$$MDT = \frac{ABC}{c_{\infty}} = \frac{\sum_{i=0}^{\infty} \left[ (c_{i+1} - c_i) * \frac{(t_i + t_{i+1})}{2} \right]}{c_{\infty}} \quad (1)$$

ABC is the area between curves, calculated by trapezoidal equation, where  $c_i$  is the release concentration of API over time  $t$ , and  $c_{\infty}$  is the initial drug load of dosage form. The 100% value of the release curve is used in the calculation because ABC does not change afterward.

The Korsmeyer-Peppas model is a semi-empirical equation to describe drug release from polymeric systems. The Korsmeyer-Peppas model can be described as the following (Equation (2))<sup>65</sup>:

$$\frac{M_t}{M_{\infty}} = k * t^n \quad (2)$$

Here,  $M_t$  and  $M_{\infty}$  are the absolute cumulative amount of drug released at time  $t$  and infinite time, respectively;  $k$  is a constant incorporating structural and geometric characteristics of the device, and  $n$  is the release exponent, indicative of the mechanism of drug release. This model has a good ability for fitting before reaching approximately 60% total amount of drug release. This model can be used to analyze the underlying release properties of the system when the mechanism is unknown or multiple release mechanism is involved. It is important to consider that the equation requires some properties of the matrix to be valid: the drug must be uniformly distributed in the matrix, with unidirectional diffusion, and the sink condition should be maintained during dissolution. Depending on the value of  $n$ , the release behavior can be classified as Fickian diffusion, abnormal transfer, or case-II transport (shown in Table 2.4)<sup>66,67</sup>.

**Table 2.4.** Characterization of the diffusion exponent  $n$  depending on the dosage form geometry.

Thin Film	Cylinder	Sphere	Drug release mechanism
0.50	0.45	0.43	Fickian diffusion
0.50 < n < 1.00	0.45 < n < 0.89	0.43 < n < 0.85	Anomalous transport

---

The next equation that was applied is Peppas-Sahlin equation (Equation (3))<sup>68</sup>.

$$\frac{M_t}{M_\infty} = k_1 \times t^n + k_2 \times t^{2n} \quad (3)$$

This equation can be used to describe the anomalous release process of drugs: the first term describes Fickian diffusion, and the second term describes Case-II relaxation contribution. The exponent  $n$  is, as in the Korsmeyer-Peppas equation, the diffusion exponent for any geometrical shape. The constants  $k_1$  and  $k_2$  describe kinetics. This equation only refers to the anomalous release of the API<sup>67</sup>.

The zero-order release equation was also applied. It refers to the constant release of a drug from a drug delivery device, independent of the drug concentration. In its simplest form, zero-order release can be expressed as (Equation (4)).

$$M_t = M_0 + k_0 t \quad (4)$$

where  $M_t$  is the cumulative amount of drug released at time  $t$ ,  $M_0$  is the initial amount of drug,  $k_0$  is the release kinetic constant.

The last equation applied is first-order release. The first order equation describes the release from the system where release rate is concentration-dependent, expressed by Equation (5)<sup>69</sup>:

$$M_t = M_0 e^{-kt} \quad (5)$$

Where  $M_t$  is the cumulative amount of drug released at time  $t$ ,  $M_0$  is the initial amount of drug,  $k$  if first-order rate constant expressed in units of time<sup>-1</sup>.



## 2.3. Results and Discussion

### 2.3.1. Preliminary study of raw materials

Thermogravimetric analysis (TGA) is an analytical technique used to determine a material's thermal stability and its fraction of volatile components by monitoring the weight change that occurs as a sample is heated at a constant rate<sup>70</sup>. All the polymer excipients showed better thermal stability than the mannitol, which did not degrade until heat above 250 °C (Figure 2.2). The process temperature was below 190 °C, meaning the drug and polymer matrix would not degrade during melting extrusion at 160 °C and 3D printing at 190 °C.

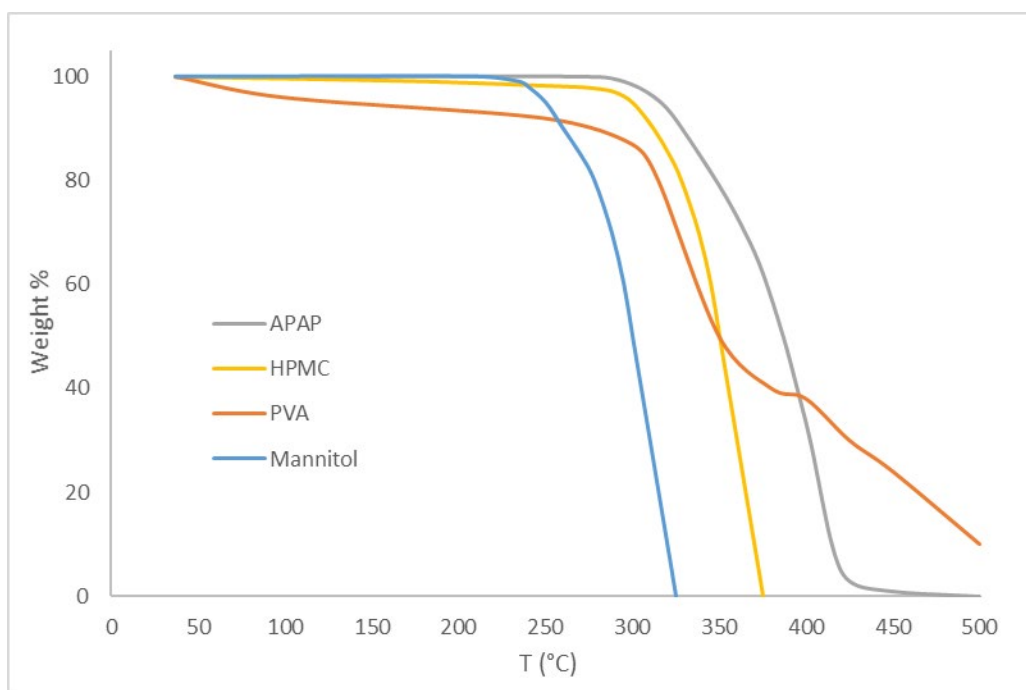


**Figure 2.2.** Thermal degradation graph of the APAP and polymer excipients.

DSC is the measurement of the change in the heat flow rate to the sample and to a reference sample while subjected to a controlled temperature program<sup>71</sup>. The APAP DSC curve exhibited a peak at 172 °C. As expected, the physical mixture showed an obvious peak at approximately 170 °C during the first heating process and no rise during the second heating process. This result indicated that APAP could disperse or dissolve into the molten polymer matrix during HME

processing, forming an amorphous solid dispersion. DSC data also showed APAP-loaded filament with HPMC 15lv matrix were amorphous (Figure 2.3).

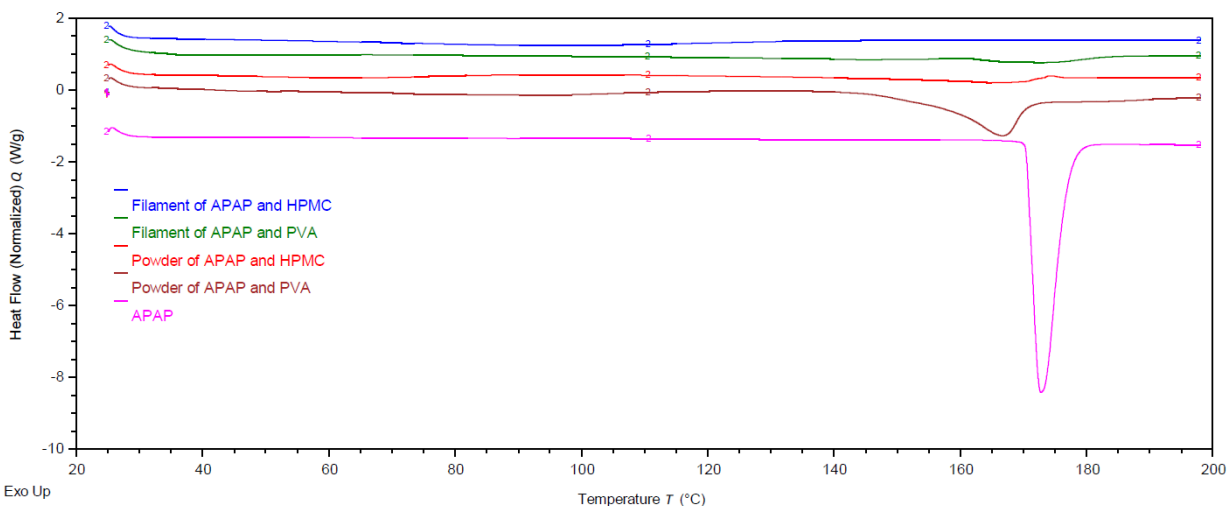


**Figure 2.3.** DSC analysis of individual polymers, extruded filaments.

### 2.3.2. Characterization of filaments

The F1, F2 filaments were successfully fabricated using hot-melt extrusion (Figure 2.4). Figure 2.4 showed that filaments of F1, F2 are semitransparent. SEM images indicated that the surface of F1, F2, and PLA are smooth and tight.

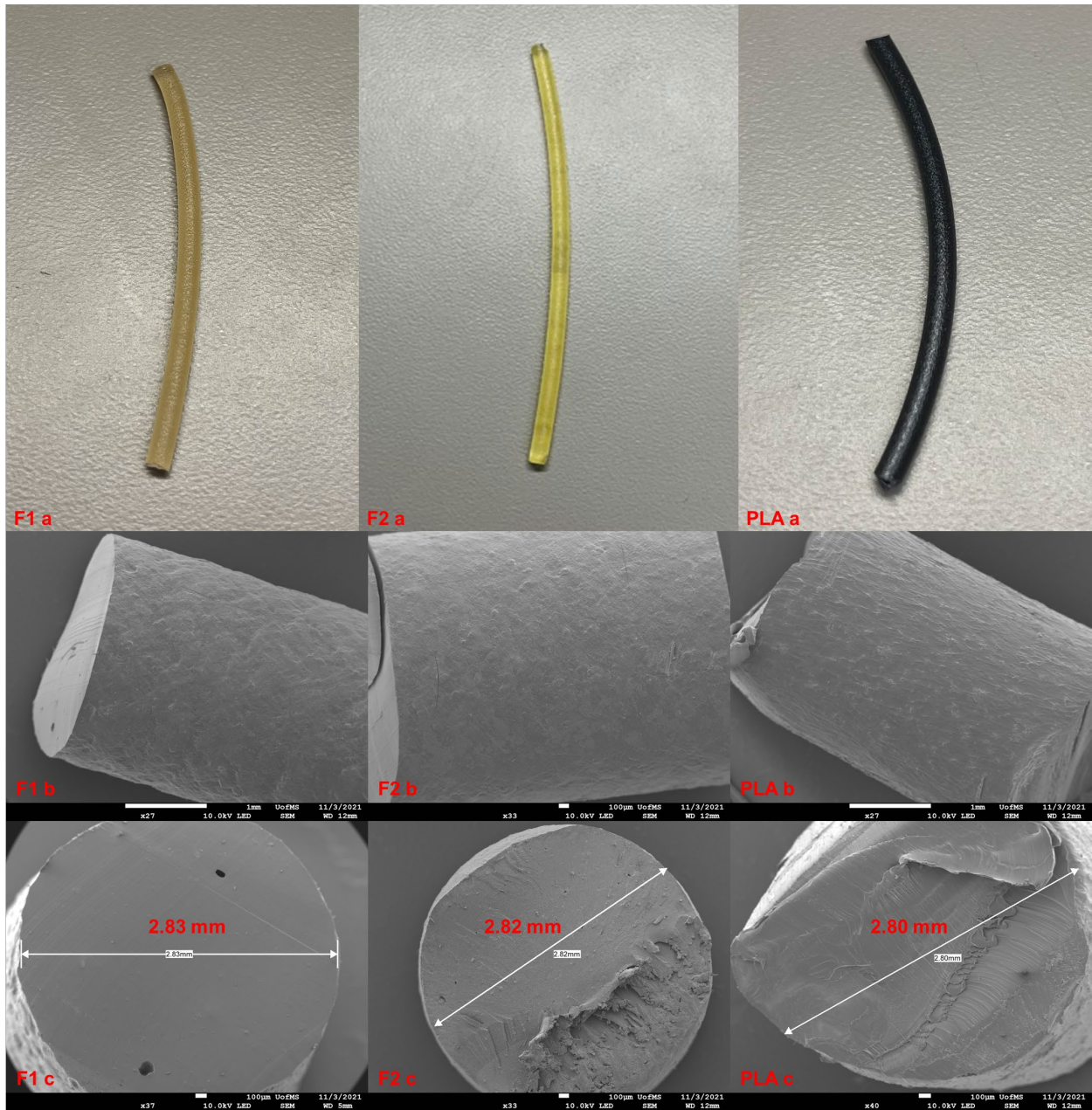


**Figure 2.4.** Photos and SEM images of F1 filament (left), F2 filament (middle) and PLA filament (right).

### 2.3.3. Mechanical Characterization of the Filaments

#### 2.3.3.1. 3PB test

An investigation into the mechanical properties of the filaments was conducted to provide an understanding of the potential printability of the filaments. The three-point bending test measured the flexural tensile strength of the filaments. Brittleness measurements were conducted for the cover filament (PLA) and the drug-loaded filaments (F1, F2) (Table 2.5).

PLA is a commercial filament with ideal mechanical properties and exhibited a high tenacity of 132.7 kg/mm<sup>2</sup>\*, a low springiness of 1.5 kg/mm<sup>2</sup>\*. On the other hand, F1 showed a lower tenacity (42.5 kg/mm<sup>2</sup>\*) but showed a higher springiness (9.1 kg/mm<sup>2</sup>\*), which means PLA was harder to bend but easier to break than F1 filament. F2 had a very low Tenacity (7.43 kg/mm<sup>2</sup>\*) and no Springiness (0 kg/mm<sup>2</sup>\*), indicating that F2 is very easy to be fractured and can barely be bent and if not feedable with existing feeding systems. Therefore, the printing of the F2 filament was feasible by adapting the feeding mechanism of the printer from feeding gears to piston feeding<sup>72</sup>.

**Table 2.5.** Texture analysis data of three filaments.

Filaments	Diameter (mm)	Three-point bend test (kg/mm <sup>2</sup> *)			Stiffness test (kg/mm <sup>2</sup> *)			Resistance test (kg/mm <sup>2</sup> *)		
		Tenacity	Springiness	Brittleness	Firmness	Resilience	Toughness	Tenacity	Springiness	Resistance
F1	2.83	42.5±0.8	9.1±0.4	51.6±1.1	60.2±2.1	45.0±2.0	105.3±4.0	19.0±0.4	1.7±0.1	20.7±0.5
F2	2.82	7.43±0.8	0	7.43±0.8	127.2±5.1	109.6±4.1	236.9±4.9	10.68±0.5	0	10.68±0.5
PLA	2.80	132.7±9.0	1.5±1.0	134.2±9.9	108.2±2.9	140.7±3.5	249.3±4.4	165.3±5.3	7.0±1.0	172.3±6.2

#### 2.3.3.2. Stiffness test

The stiffness test was applied to characterize the toughness of all filaments. As mentioned in Chapter I, toughness can predict the printability of filaments for direct drive FDM 3D printers. F2's toughness is similar to PLA's (about 240 to 245 kg/mm<sup>2</sup>\*), but F2's Firmness is greater, and

Resilience is less than PLA's, which means that F2 filament is tougher and less resilient to stress than PLA. F1 has the smallest Toughness ( $105 \text{ kg/mm}^2 \cdot \%$ ), which means the F1 filament surface hardness is the lowest, but it still far exceeded the requirements for printing.

#### 2.3.3.3. Resistance test

The resistance of filaments was measured by the resistance test. The data (Table 2.5) showed that the resistance of PLA filament was higher than F1 and F2 filaments. It means that the PLA filament will have more strength to push the fused filament to come out nozzle during the 3D printing process. Springiness of F2 is zero, which means F2 filament cannot be bent, this is consistent with that of the 3PB test results.

#### 2.3.4. Tablet morphology study

PLA filaments were selected for their good mechanical properties (Table 2.5), water resistance, and FDA approval for food contact. The covers without deformation after the dissolution test were shown in Figure 2.5.



**Figure 2.5.** Photos of covers after dissolution test.

All sixteen different structure tablets (Figure 2.5) were successfully fabricated using dual-extrusion FDM. Each tablet without cover was printed in 5-7 min depending on the structure

(Cylinder >Quad >Semi >Torus). To fabricate each tablet with cover, 15-16 min was needed (Cylinder >Quad >Semi >Torus). In the geometry study, all the tablets had small variations in weight and dimensions, which guarantee the good reproducibility of the 3D printing process. The tablets did not have physical attrition after the friability test, which means FDM tablets have a robust structure. The density of the core of tablets with cover was smaller than tablets without cover in each structure tablet. The reason for density reduction is that two nozzles need to switch frequently during every layer printing. So the frequent feed and retraction of filaments caused the weight, which leading density reduction.

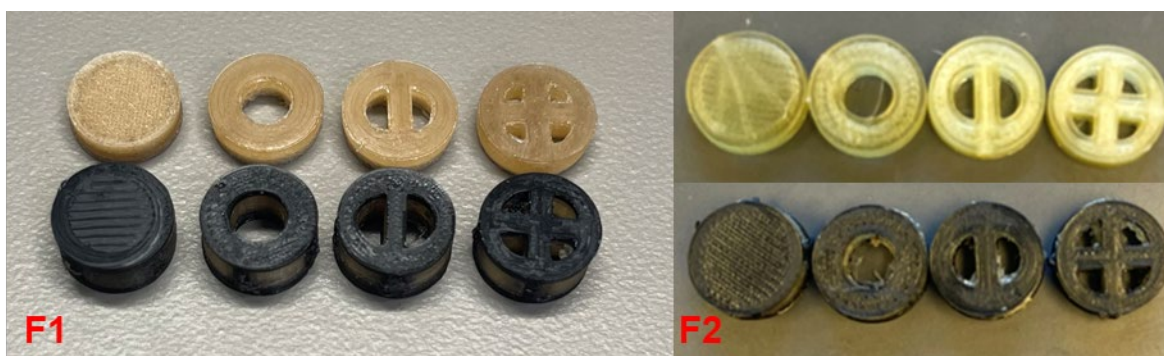


**Figure 2.6.** Photos of sixteen different structure tablets.

**Table 2.6.** Geometric characteristics of the 3D printed tablets.

Formulation		External diameter (mm)	Inner diameter (mm)	Thickness (mm)	Weight (mg)	Volume (mm <sup>3</sup> )	Density (mg/mm <sup>3</sup> )	Hardness (kp)
Cylinder		10.03 ±0.04	N/A	3.21±0.02	287.2±0.9	251	1.1	35<
Cylinder with cover	Cover	10.01 ±0.02	N/A	0.94±0.00	206.6±12.3	170	1.2	35<
	Body	10.01 ±0.02	N/A	3.22±0.02	260.6±9.5	238	1.1	
Torus		9.98 ±0.02	5.21±0.04	3.23±0.01	230.3±2.5	189	1.2	35<
Torus with cover	Cover	10.01 ±0.02	5.21±0.04	0.95±0.01	172.3±2.1	131	1.3	35<
	Body	10.01 ±0.02	5.21±0.04	3.22±0.01	177.5±0.8	176	1.0	
F1 Semi		10.02 ±0.04	5.20±0.03	3.20±0.02	228.5±11.7	189	1.2	35<
Semi with cover	Cover	10.01 ±0.04	5.22±0.02	0.96±0.01	172.7±1.7	131	1.3	35<
	Body	10.01 ±0.04	5.22±0.02	3.19±0.01	180.0±10.0	176	1.0	
Quad		10.02 ±0.03	5.21±0.02	3.20±0.02	227.0±2.5	189	1.2	35<
Quad with cover	Cover	10.0 ±0.01	5.22±0.03	0.93±0.01	173.3±2.9	131	1.3	35<
	Body	10.0 ±0.01	5.22±0.03	3.21±0.02	175.0±4.3	176	1.0	
Cylinder		10.03 ±0.04	N/A	3.21±0.02	329.7±2.1	251	1.3	35<
Cylinder with cover	Cover	10.01 ±0.02	N/A	0.94±0.00	210.3±0.9	170	1.2	35<
	Body	10.01 ±0.02	N/A	3.22±0.02	277.7±4.5	238	1.2	

	Torus		$9.98 \pm 0.02$	$5.21 \pm 0.04$	$3.23 \pm 0.01$	$258 \pm 1.6$	189	1.4	$18.3 \pm 1.2$
	Torus with cover	Cover	$10.01 \pm 0.02$	$5.21 \pm 0.04$	$0.95 \pm 0.01$	$170.7 \pm 2.1$	131	1.3	
		Body	$10.01 \pm 0.02$	$5.21 \pm 0.04$	$3.22 \pm 0.01$	$208 \pm 0$	176	1.2	$31.4 \pm 1.3$
F2	Semi		$10.02 \pm 0.04$	$5.20 \pm 0.03$	$3.20 \pm 0.02$	$261.3 \pm 0.9$	189	1.4	$22.1 \pm 1.3$
	Semi with cover	Cover	$10.01 \pm 0.04$	$5.22 \pm 0.02$	$0.96 \pm 0.01$	$170.7 \pm 4.1$	131	1.3	
		Body	$10.01 \pm 0.04$	$5.22 \pm 0.02$	$3.19 \pm 0.01$	$207.7 \pm 6.6$	176	1.2	$30.7 \pm 0.7$
	Quad		$10.02 \pm 0.03$	$5.21 \pm 0.02$	$3.20 \pm 0.02$	$263.3 \pm 1.2$	189	1.4	$24.9 \pm 1.3$
	Quad with cover	Cover	$10.0 \pm 0.01$	$5.22 \pm 0.03$	$0.93 \pm 0.01$	$173.0 \pm 6.2$	131	1.3	
		Body	$10.0 \pm 0.01$	$5.22 \pm 0.03$	$3.21 \pm 0.02$	$204.3 \pm 3.1$	176	1.2	$28.6 \pm 2.3$

### 2.3.5. *In vitro* drug release

#### 2.3.5.1 Drug release profiles

As shown in Figure 2.6, F2 (PVA-matrix) can be considered immediate-release, all kinds of tablets without PLA cover released 80% in 1 hour, the release profiles of Torus, Semi and Quad were almost the same. As for F1 (HPMC-matrix) without cover, cylinder, torus, Semi and Quad released 80% in 6h, 4h, 3.5h and 2.5h, respectively. Under PLA cover influence, F1 cylinder released 71% in 24h, torus, Semi and Quad released 80% in 8 hours, F2 cylinder, torus, Semi and Quad released 80% in 10h, 3h, 2.5h and 2h, respectively. In the same shape, Figure 2.7 showed that the release rate of tablets with cover is slower than without cover.

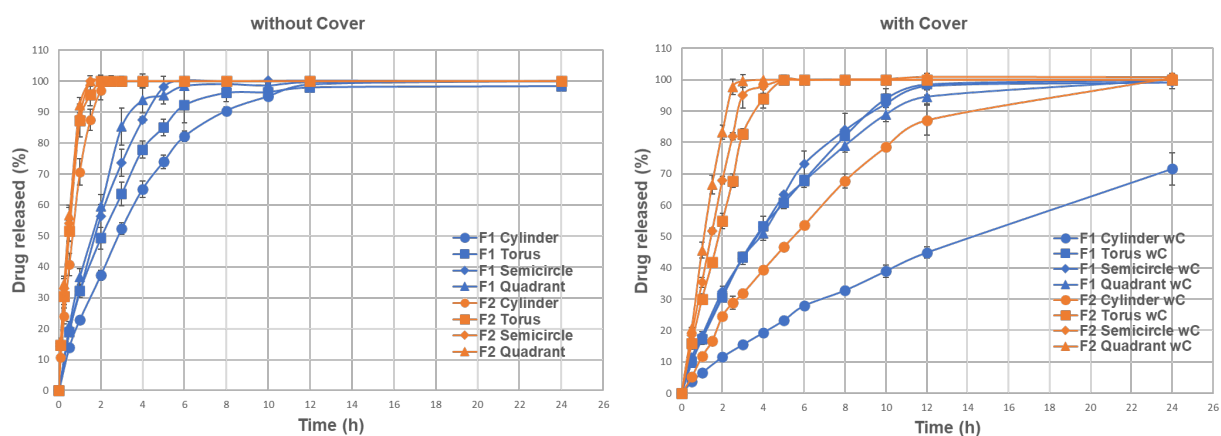


**Figure 2.7.** Dissolution profiles of different formulation and structure tablets with or without covers.

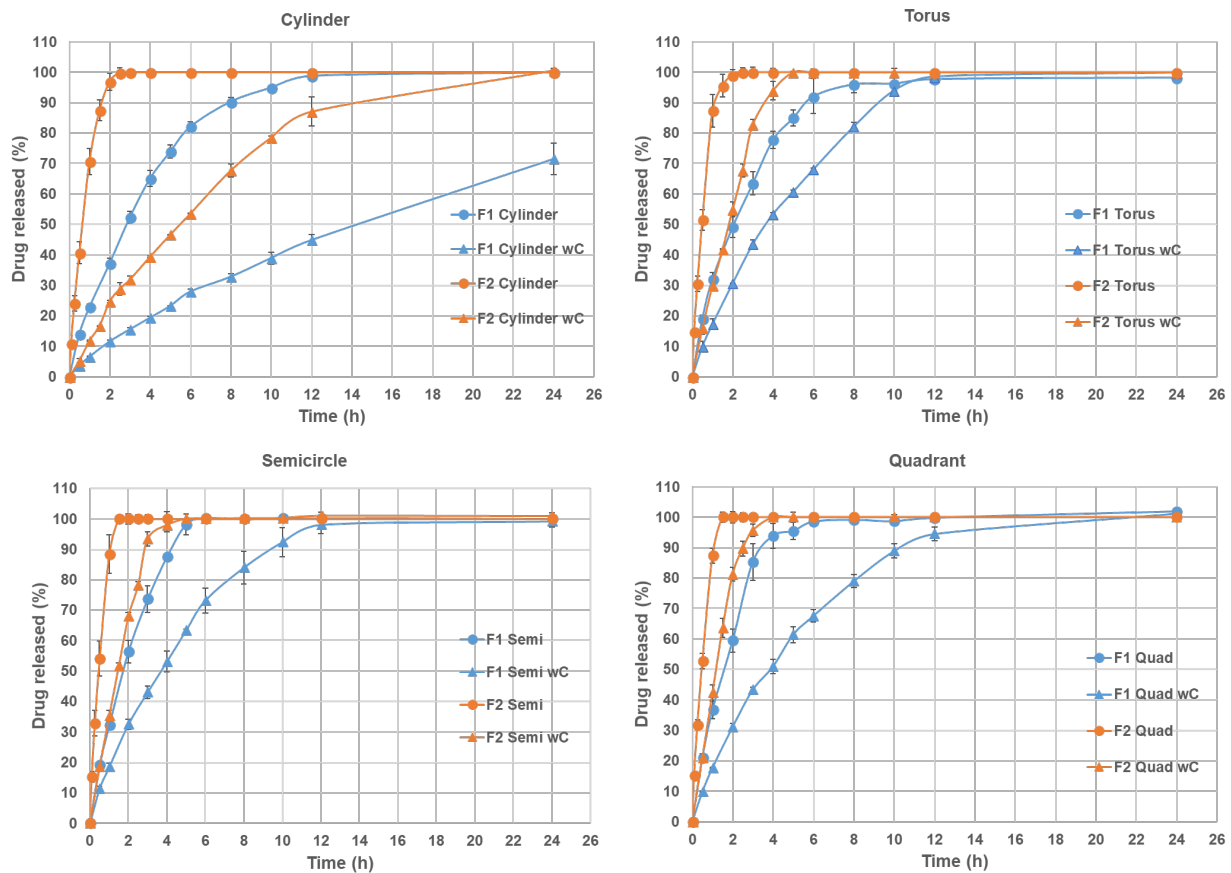


**Figure 2.8.** Dissolution profiles of same structure tablets with or without covers.

The respective MDTs were calculated using Equation (1) and listed in Table 2.7. Different geometries had different SA/V ratios. The MDT decreased with the SA/V ratio increase. Under the cover influence, each geometries' SA/V ratio decreased and MDT increased dramatically.

**Table 2.7.** MDT and SA/V ratio of each tablet.

	MDT ( $\text{h}^{-1}$ )				SA/V ratio ( $\text{mm}^{-1}$ )	
	F1 (HPMC)		F2 (PVA)		no cover	covered
	no cover	covered	no cover	covered		
Cylinder	3.62	9.94	0.76	6.71	1.03	0.42
Torus	2.34	4.50	0.56	2.52	1.43	0.86
Semi	2.01	4.40	0.52	1.53	1.59	1.04
Quad	1.70	4.96	0.49	1.29	1.76	1.22



### 2.3.5.2 Correlation between MDT and SA/V Ratio

Based on this data, a correlation between the MDT and the SA/V ratio was established. The obtained data was shown in Figure 2.8.

Without cover influences, the correlation between the variables SA/V and MDT results in a curve (Figure 2.8a) for F1 ( $MDT = 0.77*(SA/V)^{-0.83}$ ,  $R^2: 0.994$ ); F2 ( $MDT = 3.76*(SA/V)^{-1.37}$ ,  $R^2=0.999$ ). For both F1 and F2 tablets without cover, there is a good correlation between MDT and SA/V ratio. Figure 2.8a indicated that MDT of F2 without cover is not sensitive to change of SA/V ratio, which explains why the dissolution profiles of F2 Torus, Semi and Quad are similar in Figure 2.6. On the other hand, the MDT of F1 without cover is more sensitive to change of SA/V ratio, so the dissolution profiles of F1 tablets are not similar. And this correlation could be linearized by log-transformation of both axes, showed in Figure 2.8b ( $R^2: (F1 0.999), (F2 0.992)$ ). This data (Figure 2.8a, 2.8c) revealed that when tablets were not covered, the SA/V ratio influenced the relative drug release and drug release can be predicted by SA/V ratio both in immediate-release (F2) and extended-release (F1). Moreover, MDT of F1 is more sensitive to the change of SA/V ratio than F2. This prediction method had been reported by Windolf<sup>64</sup>.

When PLA covered tablets, F1 did not correlate well between drug release and SA/V ratio. But drug release of F2 had a good correlation with the SA/V ratio ( $R^2: 0.996$ ) (Figure 2.8c). The resulting curve ( $MDT = 1.78 \cdot (SA/V)^{-1.56}$ ) was linearized again via log-transformation of both axes ( $R^2: 0.994$ ). Moreover, under the cover influence, MDT of F2 became more sensitive to SA/V ratio change than uncovered F2, which explained why the dissolution profile of F2 Torus, Semi and Quad became different under the cover influence.

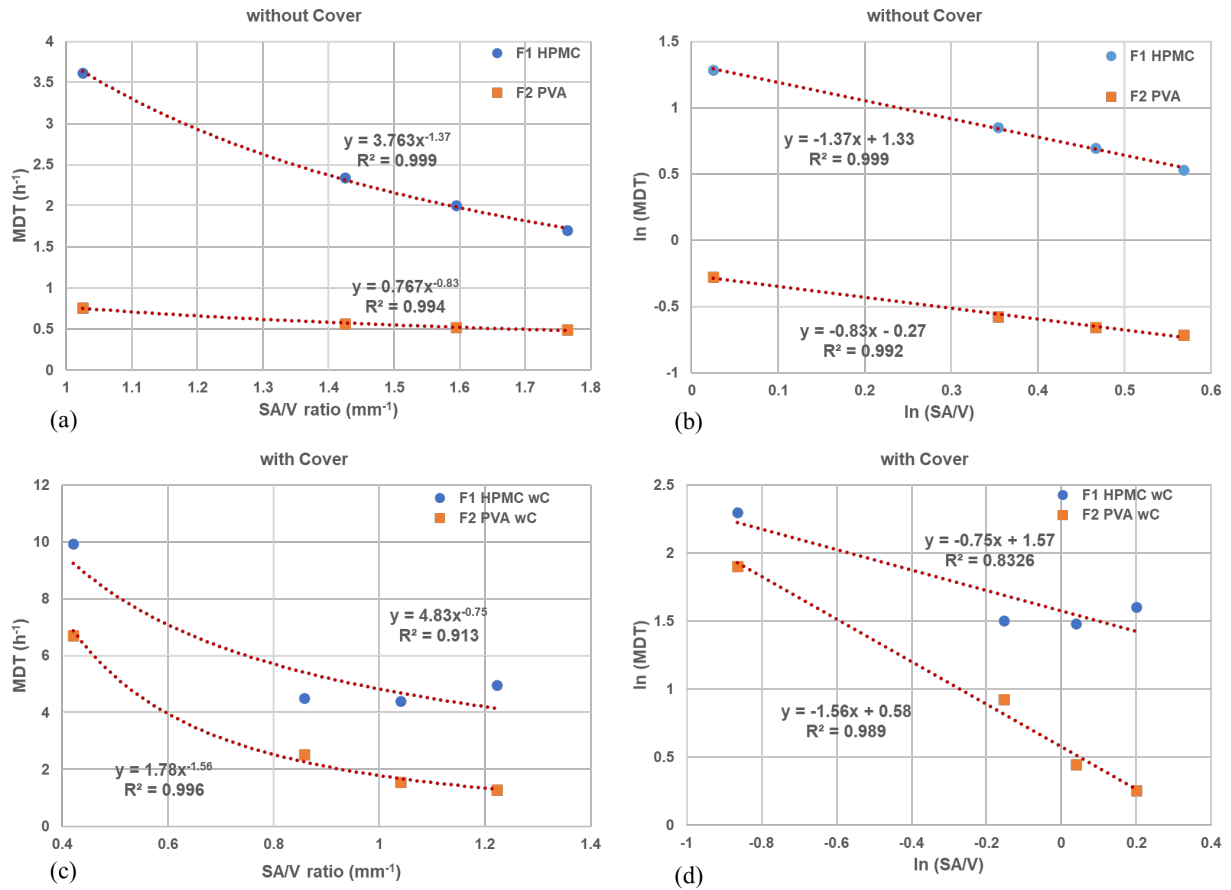


**Figure 2.9.** Correlation of MDT and SA/V ratio for F1 and F2 formulation (a, c) and linearized version (b, d).

### 2.3.5.3 Impact of geometries and PLA cover

Figure 2.9 are plots of release rate change during the dissolution process. Due to HPMC-matrix (F1) tablets having burst release phenomenon<sup>73</sup>, release rates from 20% release to 80%

were recorded in Figure 2.9a. Compared to each tablet with and without cover in F1 and F2, the release rate decreased obviously and became more steady when the tablet was covered. It means that cover can extend release time and make the dissolution profile more consistent.

In this study, the PVA matrix is a surface erosion system, the drug release from PVA-matrix was dominated by drug diffusion and matrix erosion<sup>74,75</sup>. The drug release rates of the HPMC based dosages were dominated by the 3D geometry structure and waterproof covers, the following phenomena were observed in the dissolution study:

1) A steep concentration gradient formed at the interface of medium and tablet once the tablets contacted the dissolution medium. Here, water reduced the system's glass transition temperature ( $T_g$ ) acted as a plasticizer. Once the system reached the  $T_g$  during the in vitro study, the matrix transformed to hydrogel<sup>67</sup>.

2) The HPMC-based matrix swelled and formed hydrogel while the medium was penetrating, which changed the drug concentration at the interface of the tablet and medium. The concentration gradients lead the APAP to dissolve or diffuse from the matrix to the hydrogel, thus into the dissolution medium.

3) Without PLA cover, all tablets of F1 swelled during the dissolution. Undercover influence, no apparent swell of HPMC matrix can be observed, and the structure of the PLA cover remained intact after the dissolution test.

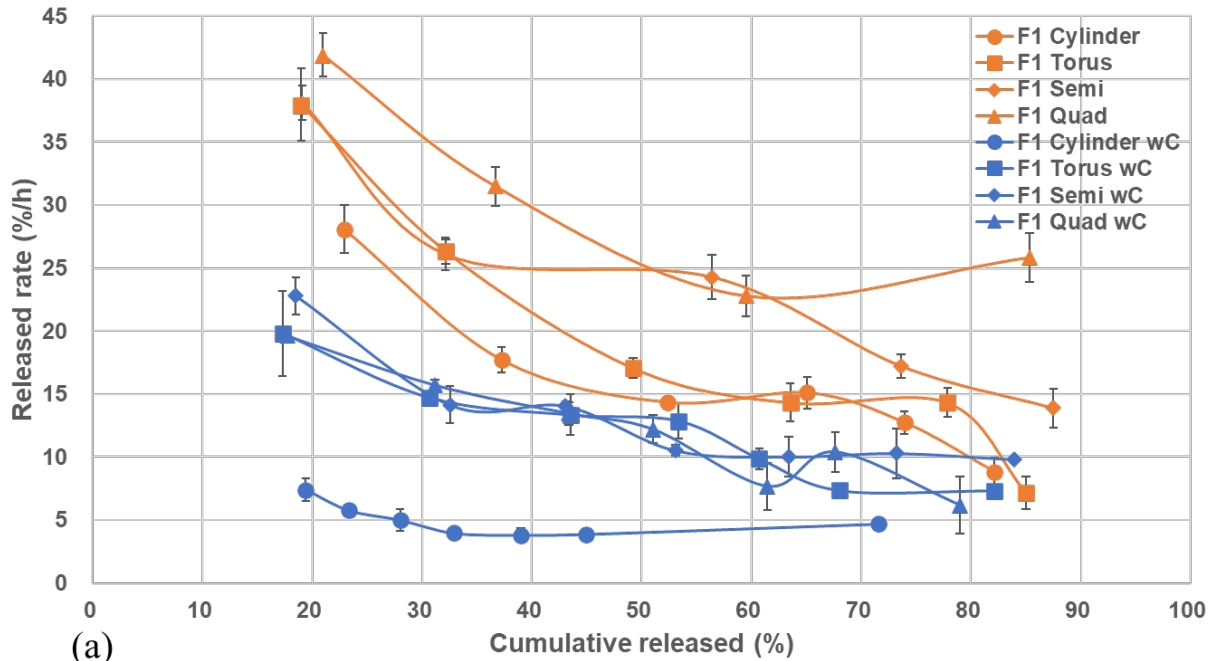
4) PVA matrix did not swell during the dissolution.

In Figure 2.9, without cover, the release rate of all PVA-matrix tablets decreased gradually. It had been mentioned before that the MDT of F2 without cover is not sensitive to the change of SA/V ratio. The reason is that the SA of Torus, Semi and Quad decreased too fast without the protection of cover. After covering, we can find that the release rate of Torus, Semi and Quad

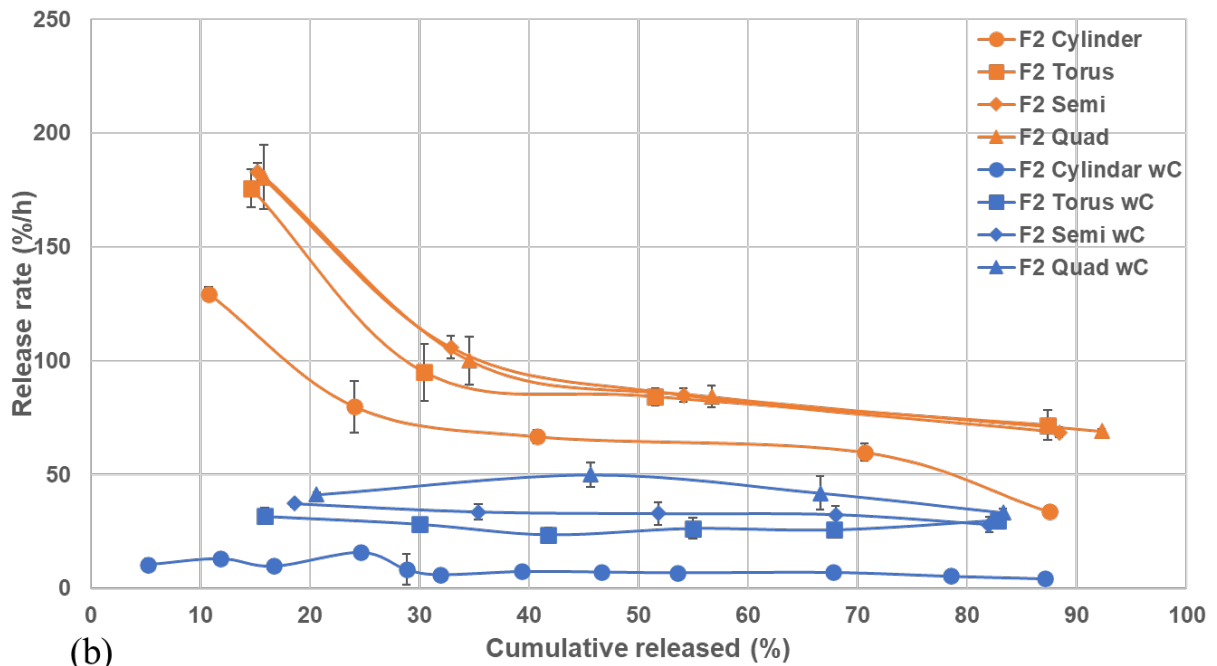
nearly did not change, like a constant, the release rate of Quad even increased, which consists with the surface area change of Quad during the dissolution.

As for HPMC-matrix, without cover, different structure tablet showed different release rates during dissolution, it is because that higher SA/V ratio means less time of water penetration whole tablets to reach dynamic equilibrium, so that without cover, MDT of F1 is very sensitive to the change of SA/V ratio. However, under the influence of cover, the release rate of Torus, Semi and Quad were almost the same, and Cylinder decreased dramatically. The reason is that cover prevent the HPMC-matrix swelling, which also means preventing the matrix from absorbing dissolution medium so that the medium penetration was prevented by the cover. Therefore, the profiles of F1 Torus, Semi and Quad release rates are similar.

After comparing the release rate changes of the tablets of two different matrices, it can be found that the release rate of the surface erosion matrix (PVA) can be manipulated by adjusting the surface area during the dissolution. For the partial bulk erosion matrix (HPMC), the release rate can be manipulated by adjusting the distance of medium penetration.



(a)



(b)

**Figure 2.10.** Plots of drug release rate change during the dissolution process, F1 (a), F2 (b).

#### 2.3.5.4 Dissolution kinetics studies

To study the drug release mechanism of tablets, four different kinetic models were employed, including Korsmeyer-Peppas, Peppas-Sahlin, zero-order, and first-order. Due to the structures of tablets in this study were not all cylinder, many kinetic models were not suitable, such

as Higuchi model. The  $R^2$  values of the fits were compared to evaluate the fit quality (Table 2.8). According to the Korsmeyer–Peppas model, the release exponent  $n$  of each tablet was obtained. Applied release exponent  $n$  to Peppas-Sahlin model,  $k_1$ ,  $k_2$  were calculated.

The drug release from the F1 (HPMC) follows an anomalous transport ( $0.65 < n < 0.79$ ). In Peppas Sahlin,  $k_2$  of all F1 tablets are negative, indicating that diffusion is predominant in the release<sup>76</sup>. The data revealed that the geometries of tablet changed release profiles of F1, Semi and Quad were more fit zero-order release than first-order. However, the PLA cover did not have much impact on the release profile of the F1. HPMC matrix needs to release the drug by swelling in the dissolution process. Since PLA cover prevented HPMC swell, the change of the geometries did not significantly influence the release profile of the covered tablet, and even the dissolution curve of the covered tablet tends to be the same (Figure 2.6).

Drug released from (F2) PVA matrix by drug diffusion and PVA surface erosion, which means release rate highly depends on the surface area. In the absence of PLA cover, the change of the geometries did not have a significant effect on F2 dissolution profiles, which all belonged to the anomalous transport ( $0.71 < n < 0.74$ ), only increasing the dissolution rate, which can be observed from MDT (Table 2.7). For surface erosion matrix tablet, cover maintained surface area of each shape tablet at a relatively constant value. According to the previous geometry design, the surface area of Cylinder with cover will decrease gradually, Torus with cover will be constant, Semi with cover will increase slowly, and Quad with cover will increase faster than Semi. From Figure 2.9, we obtained that the release rate of Cylinder with cover gradually decreased, Torus and Semi with cover were relatively constant, and Quad with cover even increased. Table 2.8 showed that after adding cover, the release exponent  $n$  of each geometry increased. The release mechanism of Torus with cover, Semi with cover, and Quad with the cover fitted Case-II transport or super

Case-II transport ( $n > 0.89$ ), which is also called zero-order release. Peppas-Sahlin model revealed that the release mechanism of F2 tablets did not change, diffusion phenomenon is predominant. Overall, the combination of PLA cover and geometry design successfully changed the release profile from anomalous transport to zero-order release by maintaining the surface area of F2 during the dissolution test.

**Table 2.8.**  $R^2$  values of model fits

	Korsmeyer-Peppas		Peppas-Sahlin			First-order	Zero-order	
	n	$R^2$	$k_1$	$k_2$	$R^2$	$R^2$	$R^2$	
F1	Cylinder	0.75	0.9991	22.3	0.25	0.9993	0.9963	0.9846
	Torus	0.65	0.9993	32.8	-0.16	0.9906	0.9958	0.9900
	Semi	0.79	0.9998	32.4	0.09	0.9998	0.9839	0.9846
	Quad	0.73	0.9994	36.2	-0.19	0.9992	0.9839	0.9977
	Cylinder wC	0.76	0.9990	7.2	-0.06	0.9993	0.9966	0.9888
	Torus wC	0.77	0.9979	18.4	-0.14	0.9976	0.9896	0.9771
	Semi wC	0.75	0.9997	19.0	0.00	0.9997	0.9923	0.9790
	Quad wC	0.76	0.9985	18.4	-0.09	0.9982	0.9967	0.9709
F2	Cylinder	0.74	0.9978	65.7	4.86	0.9999	0.9915	0.9512
	Torus	0.72	0.9970	83.0	2.40	0.9992	0.9893	0.9664
	Semi	0.71	0.9993	88.8	-0.23	0.9999	0.9862	0.9532
	Quad	0.71	0.9995	92.5	0.43	0.9999	0.9847	0.9578
	Cylinder wC	0.80	0.9884	13.3	-0.07	0.9960	0.9902	0.9496
	Torus wC	0.89	0.9969	N/A	N/A	N/A	0.9576	0.9977
	Semi wC	0.94	0.9975	N/A	N/A	N/A	0.9553	0.9951
	Quad wC	1.00	0.9985	N/A	N/A	N/A	0.9642	0.9986

## 2.4. Conclusion

All sixteen different tablets were fabricated by the FDM dual-extrusion 3D printer. Under the influence of cover, the release rate of each type of geometry tablet decreases to varying degrees and becomes more stable. Without cover, there is a highly accurate correlation of MDT and SA/V ratio, SA/V ratio increase, MDT decrease. For the surface erosion matrix (PVA), the release rate is sensitive to the SA/V ratio with cover and not sensitive to the SA/V ratio without cover, the release rate can be manipulated by adjusting the surface area during the dissolution. For the partial bulk erosion matrix (HPMC), the release rate is sensitive to the SA/V ratio without cover and not

sensitive to the SA/V ratio with cover, the release rate can be manipulated by adjusting the distance of water penetration. The release profiles of dosages containing APAP and HPMC or PVA polymer matrix had been manipulated by applying the combination of PLA cover and geometry design via 3D printing technologies.



## **CHAPTER III**

### **DEVELOPMENT OF TWO-API PULSATILE RELEASE ORAL TABLETS WITH FOUR LAYERS STRUCTURE BY 3D PRINTING TECHNOLOGY**

#### **3.1 Introduction**

Pulsatile drug delivery system (PDDS) is defined as the rapid and transient release of a certain amount of molecules within a short time period immediately after a predetermined off-released period. PDDS is time and site-specific drug delivery, providing spatial and temporal delivery and improving patient compliance<sup>77-80</sup>.

Humans exhibit endogenous circadian rhythms, regulated by the body's master clock. Chronic pathologies with circadian symptoms, such as cardiovascular disease, bronchial asthma, rheumatoid arthritis, and sleep disorders, are most likely to recur at night or early in the morning. Treatment of such diseases requires pulsatile drug delivery systems, by which the drug is released rapidly and entirely as a pulse after a lag time. In addition to chronic pharmaceutical purposes, oral time-based pulsatile release systems can be used to achieve colon delivery if the dosage form is enteric coated to overcome unpredictable gastric residence<sup>81,82</sup>. In the oral delivery area, the colonic release is a major focus of research mainly because of its established benefits in the therapy of inflammatory bowel disease and its potential as a release site for peptide drugs, which generally show oral bioavailability issue<sup>83</sup>.

There are many advantages of PDDS. Some of them are listed below: 1. It can be used to prolong daytime or nighttime activities. 2. Can reduce the dose frequency, which can improve patient compliance. 3. Drugs can be adapted to suit the circadian rhythms of diseases or body functions. 4. Site-specific drugs, such as the colon, can be achieved. 5. Can prevent drug loss by

extensive first-pass metabolism. 6. Constant plasma concentration at the site of action can be achieved<sup>84,85</sup>.

Although the first PDDS was devised as multi-layer tablets in the impermeable shell, oral bioactive compounds' timing release is currently achieved by applying functional polymeric coatings at the drug-containing core. Accordingly, erodible, rupturable, permeable and semipermeable layers can be distinguished. The traditional oral PDDS with polymeric coating still had some disadvantages: 1. Low drug loading capacity and incomplete release of the drug. 2. Multiple manufacturing steps<sup>86</sup>.

Hot-melt extrusion (HME) technology has been developed and applied in pharmaceutical manufacturing for 20 years and is probably the best method for preparing polymeric formulations with a high drug load<sup>9</sup>. A double-rotor extruder is mainly used to process soluble polymers and soluble/insoluble drugs, which are mixed at the same time of melting. Part or all drugs are dissolved into the polymer matrix, forming amorphous solid dispersions with improved bioavailability and stability<sup>87</sup>.

In order to fabricate complex structure PDDS with fewer manufacturing steps, fused deposition modeling (FDM) 3D printing technology was applied. FDM 3D printing is a method of additive manufacturing where layers of materials are fused in a pattern to create an object. The material is melted just past its glass transition temperature and then extruded in a pattern next to or on top of previous extrusions, creating an object layer by layer. Compared to the conventional tablets manufacturing technique, 3D printing offers high flexibility and complexity in design release profiles and tablet structures<sup>88-90</sup>. The combination of HME and FDM technologies has great potential to overcome the disadvantage of traditional oral PDDS.

This study aimed to couple FDM 3D printing with HME technology to fabricate two-APIs oral PDDS and investigate the correlation between structure and release profiles.

## 3.2 Materials and Methods

### 3.2.1. Materials

Acetaminophen (APAP; Spectrum Chemical, New Brunswick, NJ, USA) and Caffeine citrate (CC) (Pfaltz & Bauer, Waterbury, CT, USA) were selected as model drugs. APAP and caffeine citrate are both BCS class I (high solubility). The melting point of APAP and caffeine citrate are 169-170 °C and 159-161°C, respectively<sup>60,91</sup>. Affinisol HPMC HME 15LV was graciously donated by Colorcon (PA, USA). For dissolution medium preparation, potassium phosphate monobasic and sodium hydroxide were purchased from Jost Chemical (MO, USA) and J.T.Baker, PA, USA, respectively.

### 3.2.2. Formulation and preparation of filaments

Two different formulations were tried in this study (Table 3.1) To get a physical mixture, raw materials were mixed on a Maxiblend™ (GlobePharma, New Brunswick, NJ, USA) at 25 rpm for 30 min, after filtration through a US #30 mesh screen to remove any aggregates that may have formed.

A co-rotating, twin-screw extruder with 11 mm diameter screws, L/D of 40, and eight electrically heated zones (Thermo Fisher Scientific, Waltham, MA, USA) was applied in this study. Physical mixtures were extruded with a standard screw configuration at screw speed 50 RPM. The molten materials were extruded through a 2.5 mm round shape die and a conveyor belt was used to control the diameter of filaments (2.6-2.85 mm).

**Table 3.1.** Operation parameters for the two different formulations during the HME process.

Formulations	API (w/w) %	Polymer (w/w) %	T (°C)	Torque (N*m)	Pressure (bar)
F1	20% APAP	80% HPMC	155	6.8	44
F2	20% Caffeine citrate	80% HPMC	145	6.0	35

### 3.2.3. Thermogravimetric analysis (TGA)

During HME processing, a PerkinElmer Pyris 1 TGA calorimeter was used to determine the thermal stability of caffeine citrate. The samples were placed in an open aluminum pan and heated from 30 to 500 °C at a rate of 20 °C/min. Ultra-purified nitrogen was used as the purge gas at a flow rate of 25 mL/min. Data were collected and analyzed using Pyris software, and percentage mass loss and/or onset temperatures were calculated.

### 3.2.4. Differential scanning calorimetry (DSC)

The drug crystallinity and characterize drug miscibility in the extrudates were studied by a differential scanning calorimeter (Discovery DSC, TA Instruments, USA). Samples (5-10 mg) were sealed in an aluminum pan and heated from 40 to 200 °C at a rate of 10 °C/min. Ultra-purified nitrogen was used as the purge gas at a 50 mL/min flow rate in all DSC experiments. Data were collected and analyzed using the Trios Data Analysis software (TA Instruments). All melting temperatures are reported as extrapolated onset unless otherwise noted.

### 3.2.5. Mechanical characterization of filaments

Three different texture analysis methods, using TA. XTPlus (Stable Micro Systems Ltd, Godalming, Surrey, UK) were used to determine the mechanical properties of filaments. The three-point bending (3PB), stiffness, and resistance tests were employed to measure the brittleness, stiffness and resistance of filaments, respectively.

### 3.2.6. Design of 3D models

The models of all tablets were designed by Fusion 360 (Autodesk, Mill Valley, CA, USA) and were sliced by Ultimaker Cura software (version 4.10; Ultimaker, Geldermalsen, The Netherlands). Figure 3.1 is the image of different structure tablets. The diameter of the kind of tablet is 10mm and the thickness is 5mm. Each tablet consists of four layers. The thickness of each layer is equal to half the diameter of this layer. Yellow layers are made of F1; red layers are made of F2. The volume ratio of each layer from the outside in is 1:1:1:1 (Figure 3.1a), 2:2:1:1 (Figure 3.1b) and 4:2:2:1 (Figure 3.1c), respectively. The diameter and volume of each layer in three kinds of tablets were shown in Table 3.2.



**Figure 3.1.** The 3D designed models of pulsatile-released tablets. a) 1:1:1:1 ratio of volume; b) 2:2:1:1 ratio of volume (outside in); c) 4:2:2:1 ratio of volume

**Table 3.2.** The parameters of each layer of three tablets

Volume ratio	d4 (mm)	d3 (mm)	d2 (mm)	d1 (mm)	V4 (mm <sup>3</sup> )	V3 (mm <sup>3</sup> )	V2 (mm <sup>3</sup> )	V1 (mm <sup>3</sup> )
1111	6.3	7.94	9.09	10	98.2	98.2	98.2	98.2
2211	5.5	6.93	8.74	10	65.4	65.4	130.9	130.9
4221	4.81	6.93	8.22	10	43.6	87.3	87.3	174.5

\*Thickness =  $\frac{1}{2}$  Diameter

### 3.2.7. 3D printing

Tablets were fabricated from the extruded filaments (yellow layer: F1 filament, red layer: F2 filaments) by an Ultimaker 3S printer (Ultimaker, Geldermalsen, The Netherlands) with two

extruders, which had two 0.4 mm nozzles. The parameters of the printing process were shown in Table 3.3.

**Table 3.3.** The parameters of 3D printing process.

Extruders	Extruder 1	Extruder 2
Filaments	F1	F1
Printing part	Yellow layer	Red layer
Layer height (mm)	0.1	0.1
Shell thickness (mm)	0.4	0.4
Infill pattern and density	Lines, 100%	Lines, 100%
Print speed, Pattern speed (mm/s)	40,18	40, 18
Printing temperature (°C)	190	185
Building plate temperature (°C)	60	60

### 3.2.8. Assessment of tablet morphology

#### 3.2.8.1. Assessment of tablet morphology

The diameter and thickness of tablets were determined by A VWR1 digital caliper (VWR1, PA, U.S.). An iPhone 12 Pro Max (Apple, Cupertino, CA) took images of the tablets.

#### 3.2.8.2. Determination of tablet strength

A standard tablet hardness tester (VK200; Agilent Technologies, Santa Clara, CA, USA) tested the tablets with a maximum force of 35 kp. Six tablets from each group of tablets were tested.

### 3.2.9. In vitro drug release study

The United States Pharmacopeia (USP) dissolution apparatus II (Hanson SR8-plus™; Hanson Research, Chatsworth, CA, USA) was applied to determine the drug release from different 3D structured tablets. Dissolution tests were conducted as per US Pharmacopeia standards using Simulated Intestinal FluidTS (without pancreatin, pH 6.8), which is representative of the small intestinal fluid of humans. Each experiment was carried out in triplicate using 900 mL of dissolution medium at  $37 \pm 0.5$  °C for 24 h. The paddle speed was set at 50 RPM. Sinkers were used to keep the tablets submerged in the dissolution vessel. The amount of released APAP and

caffeine citrate were determined by HPLC (Waters Corp., Milford, MA, USA) at 243 nm and 265 nm analyzed using Empower software (version 2, Waters Corp.).

### 3.3 Results and Discussion

#### 3.3.1. Preliminary study of raw materials

Thermogravimetric analysis (TGA) was used to determine a material's thermal stability and its fraction of volatile components by monitoring the weight change that occurs as a sample is heated at a constant rate. Figure 3.2 only showed the thermal stability of caffeine citrate due to other materials used in this chapter that had been tested in previous chapters. Caffeine citrate did not degrade until heat above 250 °C, which means the caffeine citrate and polymer matrix would not degrade during melting extrusion at 145 °C and 3D printing at 185 °C.

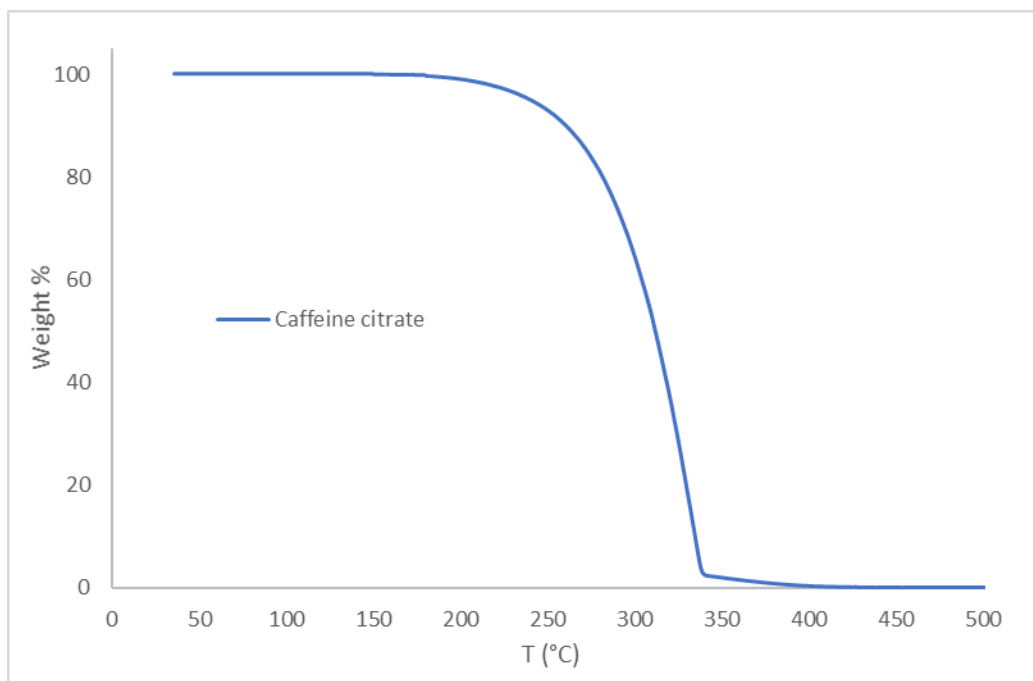


**Figure 3.2.** Thermal degradation graph of the APAP and polymer excipients.

The previous DSC studies had shown the result of APAP, powder of APAP and HPMC, and filament of APAP and HPMC. Therefore, only the DSC data analysis of CC was analyzed

here. The CC DSC curve exhibited a peak at 163°C. The physical mixture of CC and HPMC showed an obvious peak at approximately 145°C. DSC data also showed filament of CC and HPMC were amorphous.

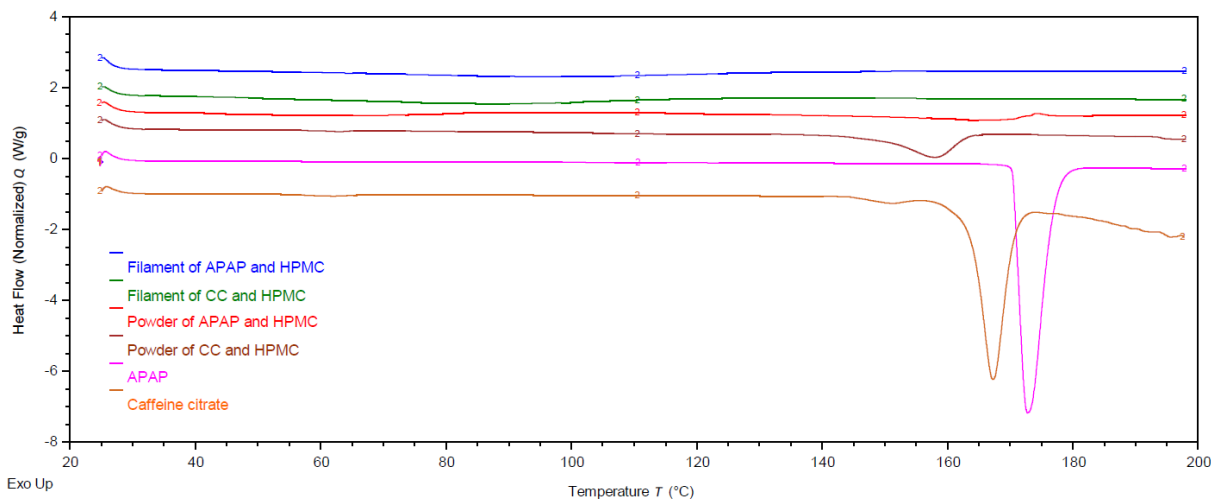


**Figure 3.3.** DSC analysis of API, physical mixture, extruded filament.

### 3.3.2. Characterization of filaments

The filaments of F1 and F2 were successfully fabricated by the HME technology. The appearances of the two filaments did not have many differences, and the color of F1 and F2 filaments are both faint yellow and semi-transparent.

The mechanical properties of the two filaments are shown in Table 3.4. The diameter of the two filaments was uniform and around 2.85 mm. Texture analysis data revealed that the physical properties of CC-loaded filament are better than APAP-loaded filament in all aspects. However, the previous chapter indicated that the mechanical properties of F1 were good enough to meet 3D printing requirements.

**Table 3.4.** Texture analysis data of three filaments.

Filaments	Diameter (mm)	Three-point bend test (kg/mm2*%)			Stiffness test (kg/mm2*%)			Resistance test (kg/mm2*%)		
		Tenacity	Springiness	Brittleness	Firmness	Resilience	Toughness	Tenacity	Springiness	Resistance
F1	2.83	42.5±0.8	9.1±0.4	51.6±1.1	60.2±2.1	45.0±2.0	105.3±4.0	19.0±0.4	1.7±0.1	20.7±0.5



### 3.3.3. Tablet morphology study

Tablets were characterized to ensure the printing quality (Table 3.5). The printing precision is considered very good for all three kinds of tablets, and the deviation is very low, which guarantees good reproducibility. The hardness of all tablets was beyond the maximum load of equipment (35 kp), which indicates the FDM tablets were physically robust.

**Table 3.5.** Geometry study of the tablets.

Ratio of Volume	Diameter (mm)	Thickness (mm)	Volume (mm <sup>3</sup> )	Weight (mg)	Density (mg/mm <sup>3</sup> )	Hardness (kp)
1111	10.05±0.06	5.05±0.03	400.34	478.33±1.70	1.19	>35
2211	10.10±0.11	5.06±0.04	404.87	463.00±1.41	1.14	>35
4221	10.13±0.08	5.04±0.04	405.66	467.00±8.52	1.15	>35

### 3.3.4. *In vitro* drug release study

As figure 3.4 shows, all drug release profiles have an off-release period at a certain time, which fits the definition of PDDS. The release of CC in each tablet had a certain delay time, depending on the thickness of the outermost (first) layer. The start release time of CC can be roughly calculated by using the initial speed of CC release and the first release point. The Correlation between first layer thickness and CC start release time in a curve (Figure 3.5a) (Start time =  $3.34 * (\text{Thickness})^{1.8}$ , R<sup>2</sup>: 0.9999). And this correlation could be linearized by log-transformation of both axes, showed in Figure 3.5b (R<sup>2</sup>= 0.9999). This correlation revealed that the start release time point of CC is influenced by first layer thickness, and the thickness of the first layer can predict the CC start release time point.

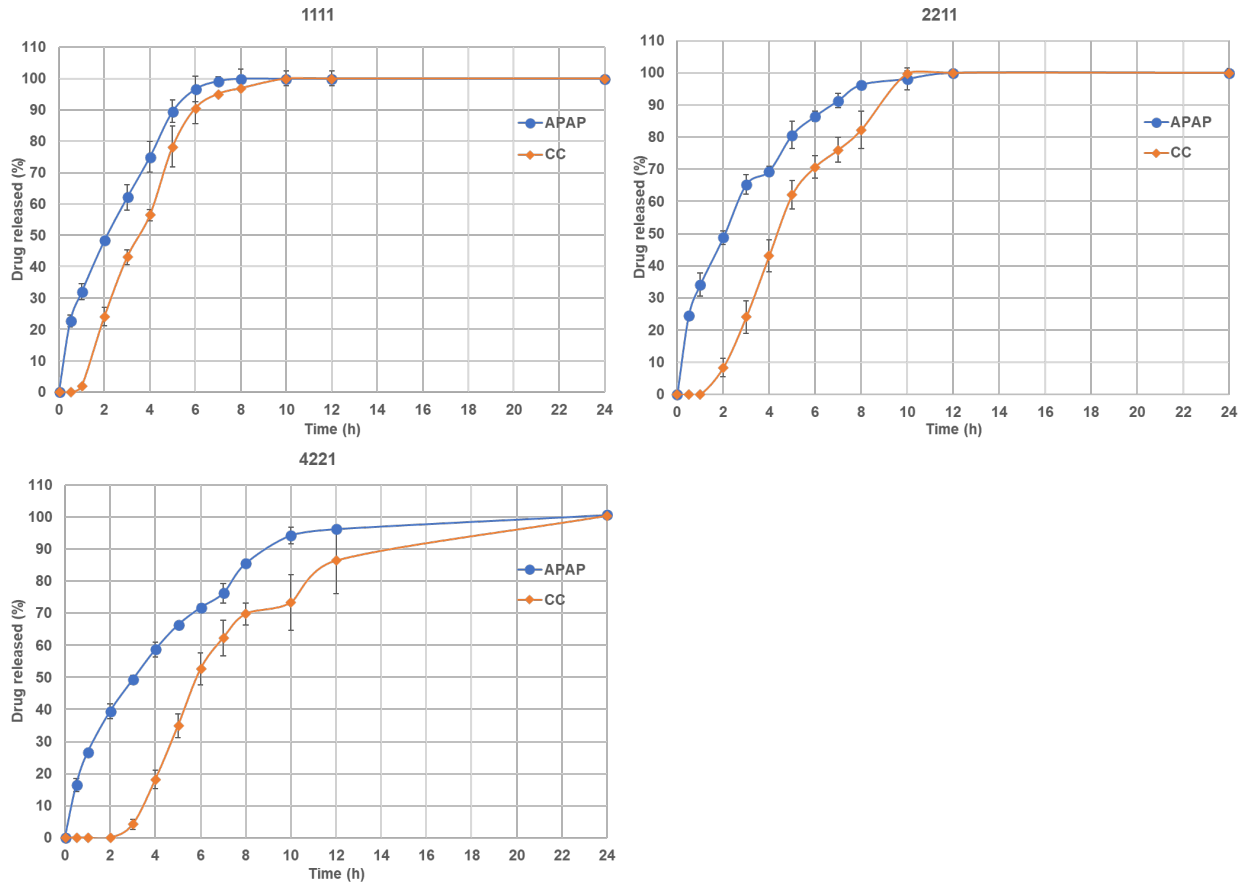


**Figure 3.4** *In vitro* drug release profiles of tablets with the different volume ratios of each layer.

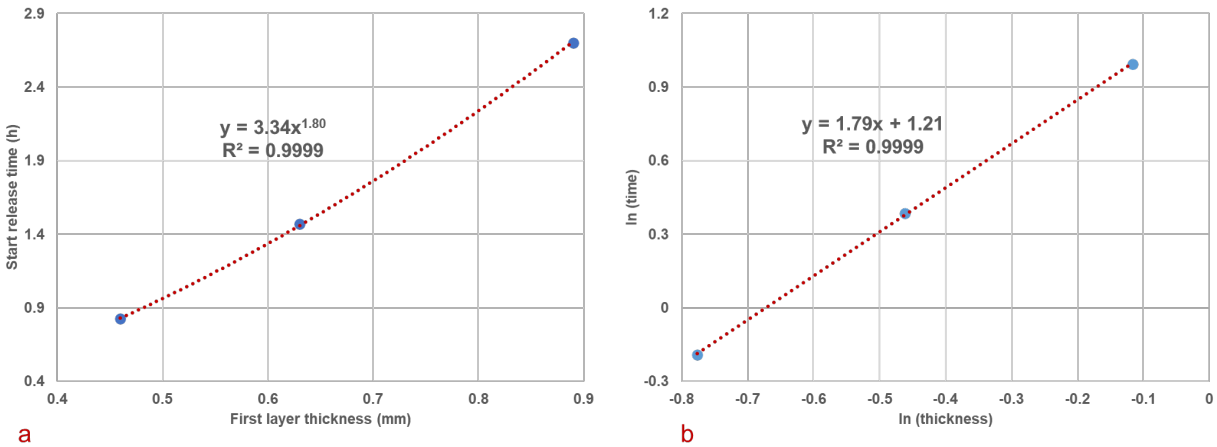


**Figure 3.5.** Correlation of start release time of CC and thickness of the first layer (a) and linearized version (b).

The release rate change of each tablet during the dissolution process had shown in Figure 3.6. The data revealed that the release rate of APAP and CC in each tablet decreased first, then

increased, finally decreased still 100% drug release. APAP and CC had an off-release period in each tablet and then had a rapid and transient release, which is in line with the definition of PDDS. In equal volume ratio tablet, APAP off-release period showed at 4h, when APAP released 75.6%. The off-release period of CC happened at 4h, and CC released 56.5% at that time. As for the “2211” tablet, the off-release period of APAP and CC occurred at 4h and 7h, at that time, APAP and CC released 69.5% and 76%, respectively. For the “4221” tablet, the APAP and CC off-release periods occurred at 7 and 10 hours, respectively, when the APAP and CC released 76.2% and 73.3%, respectively. The dissolution mechanism of HPMC includes erosion, diffusion, and swelling. The dissolution medium will penetrate the HPMC matrix and form hydrogel at the surface of the matrix and medium. The medium penetration may be why the first stage APAP and CC released beyond the predetermined percent of drug release.

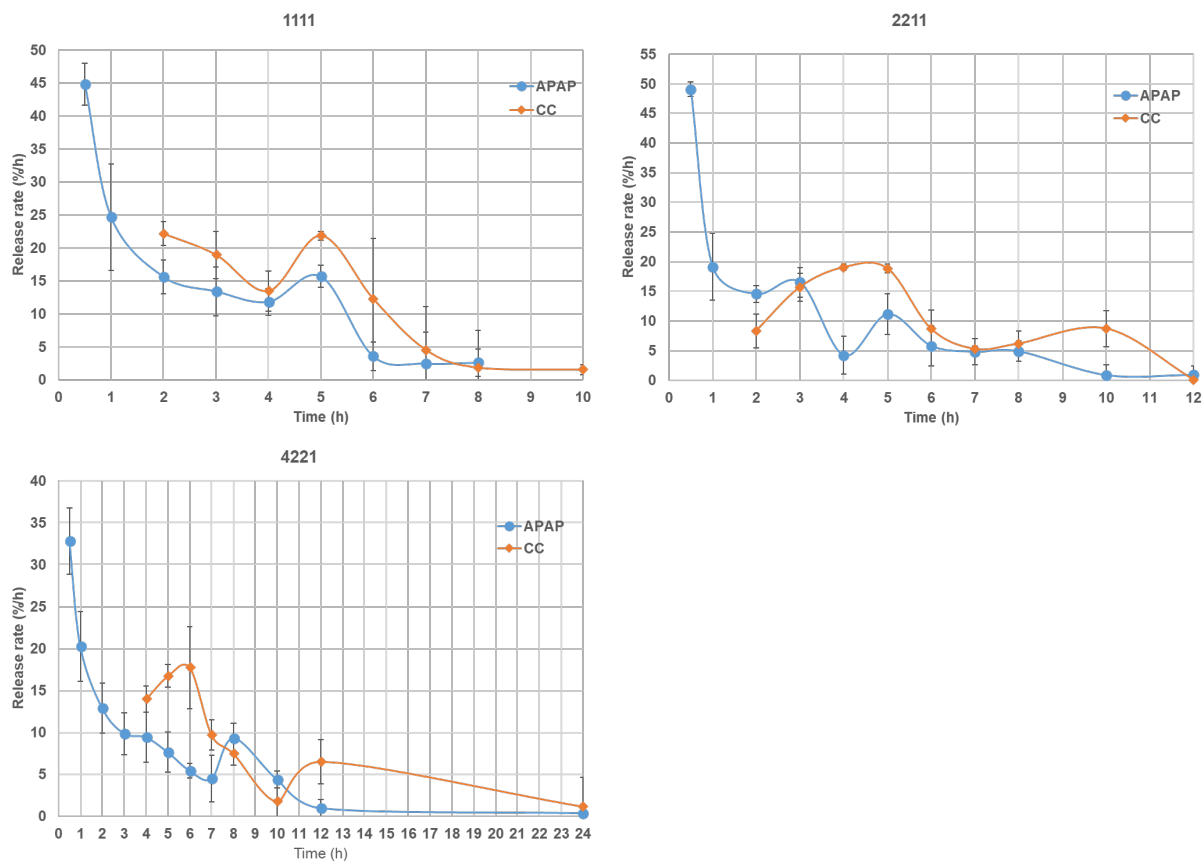


**Figure 3.6.** Release rate of each tablet during the dissolution test.

### **3.4 Conclusion**

In this study, two different drug-loaded filaments were successfully extruded. The texture analysis data showed that two drug-loaded filaments had good mechanical properties, which was enough for 3D printing. Three different kinds of two-APIs HPMC-matrix four layers tablets were successfully fabricated. All FDM tablets were robust and had very low deviations in diameter and thickness. The dissolution study showed that three kinds of tablets all have an off-release period, which fitted the definition of PDDS. The CC delay released time had corresponded with the thickness of the first layer, and the thickness of the first layer can predict the CC delay released time. The dissolution mechanism of HPMC polymer should be the reason why the APAP and CC were released in the first stage beyond the predetermined percent of drug release.

## CONCLUSION

The recent development of complex patient-focused has interested regulatory bodies. Academic and industrial researchers have investigated HME-based FDM 3D printing for dosage form fabrication. This process could be an efficient and economical method for the development of patient-focused drug products<sup>92</sup>.

The report of “Research And Markets” revealed that the global market revenue generated by AM accounts for USD 12 Billion in the year 2020, and it is anticipated to reach around USD 78 Billion by the year 2028. The market growth dynamics account for around 26%- 32% CAGR during the forecast period, 2020-2028. This suggests a huge market potential for additive manufacturing in the near future.

In order to develop FDM technology, efforts still need to be made in three aspects. More suitable printing materials need to be developed, which means good mechanical properties and miscibility. Developing more accurate and multi-functional 3DP machines, decreasing the process window so that more complex structures can be printed with more materials, and even combining HME and FDM in one device. The third point is that researchers need to do more innovative research. After all, in 3D printing, anything is possible.

In this dissertation, an economical and efficient platform was developed by combining the texture analyzer, FDM, and HME technologies to fabricate oral patient-focused 3D printed tablets. The screening printable filaments and fabrication of the zero-order release, first-order release, and two-APIs pulsatile release tablets can be achieved in this platform, and dissolution profiles can be manipulated.

## References

1. Tiwari G, Tiwari R, Bannerjee S, et al. Drug delivery systems: An updated review. *Int J Pharm Investig.* 2012;2(1):2. doi:10.4103/2230-973x.96920
2. Santos HA, Salonen J, Bimbo LM, Lehto VP, Peltonen L, Hirvonen J. Mesoporous materials as controlled drug delivery formulations. *J Drug Deliv Sci Technol.* 2011;21(2):139-155. doi:10.1016/S1773-2247(11)50016-4
3. Gross BC, Erkal JL, Lockwood SY, Chen C, Spence DM. Evaluation of 3D printing and its potential impact on biotechnology and the chemical sciences. *Anal Chem.* 2014;86(7):3240-3253. doi:10.1021/ac403397r
4. Norman J, Madurawe RD, Moore CMV, Khan MA, Khairuzzaman A. A new chapter in pharmaceutical manufacturing: 3D-printed drug products. *Adv Drug Deliv Rev.* 2017;108:39-50. doi:10.1016/j.addr.2016.03.001
5. Sachs E, Cima M, Williams P, Brancazio D, Cornie J. Three dimensional printing: Rapid tooling and prototypes directly from a CAD model. *J Manuf Sci Eng Trans ASME.* 1992;114(4):481-488. doi:10.1115/1.2900701
6. Fina F, Goyanes A, Rowland M, Gaisford S, Basit AW. 3D printing of tunable zero-order release printlets. *Polymers (Basel).* 2020;12(8). doi:10.3390/polym12081769
7. Dumpa N, Butreddy A, Wang H, Komanduri N, Bandari S, Repka MA. 3D printing in personalized drug delivery: An overview of hot-melt extrusion-based fused deposition modeling. *Int J Pharm.* 2021;600(December 2020):120501. doi:10.1016/j.ijpharm.2021.120501
8. Alhnan MA, Okwuosa TC, Sadia M, Wan KW, Ahmed W, Arafat B. Emergence of 3D

Printed Dosage Forms: Opportunities and Challenges. *Pharm Res.* 2016;33(8):1817-1832.

doi:10.1007/s11095-016-1933-1

9. Sarode AL, Sandhu H, Shah N, Malick W, Zia H. Hot melt extrusion (HME) for amorphous solid dispersions: Predictive tools for processing and impact of drug-polymer interactions on supersaturation. *Eur J Pharm Sci.* 2013;48(3):371-384. doi:10.1016/j.ejps.2012.12.012
10. Sareen S, Joseph L, Mathew G. Improvement in solubility of poor water-soluble drugs by solid dispersion. *Int J Pharm Investig.* 2012;2(1):12. doi:10.4103/2230-973x.96921
11. Aulton ME, Taylor K. *Aulton's Pharmaceutics : The Design and Manufacture of Medicines.* Churchill Livingstone/Elsevier; 2013.
12. Wei C, Solanki NG, Vasoya JM, Shah A V., Serajuddin ATM. Development of 3D Printed Tablets by Fused Deposition Modeling Using Polyvinyl Alcohol as Polymeric Matrix for Rapid Drug Release. *J Pharm Sci.* 2020;109(4):1558-1572. doi:10.1016/j.xphs.2020.01.015
13. Norman J, Madurawe R, ... CM-A drug delivery, 2017 undefined. A new chapter in pharmaceutical manufacturing: 3D-printed drug products. *Elsevier.* Accessed February 3, 2020. <https://www.sciencedirect.com/science/article/pii/S0169409X16300771>
14. Fuenmayor E, Forde M, Healy A V., et al. Material considerations for fused-filament fabrication of solid dosage forms. *Pharmaceutics.* 2018;10(2):1-27. doi:10.3390/pharmaceutics10020044
15. Alhnan MA, Okwuosa TC, Sadia M, Wan KW, Ahmed W, Arafat B. Emergence of 3D Printed Dosage Forms: Opportunities and Challenges. *Pharm Res.* 2016;33(8):1817-1832. doi:10.1007/s11095-016-1933-1
16. Morsy R, Hosny M, Reicha F, Elnimr T. Developing and physicochemical evaluation of cross-linked electrospun gelatin–glycerol nanofibrous membranes for medical applications.



- J Mol Struct.* 2017;1135:222-227. doi:10.1016/J.MOLSTRUC.2017.01.064
17. Nasereddin JM, Wellner N, Alhijaj M, Belton P, Qi S. Development of a Simple Mechanical Screening Method for Predicting the Feedability of a Pharmaceutical FDM 3D Printing Filament. *Pharm Res.* 2018;35(8). doi:10.1007/s11095-018-2432-3
  18. Crowley MM, Zhang F, Repka MA, et al. Pharmaceutical applications of hot-melt extrusion: Part I. *Drug Dev Ind Pharm.* 2007;33(9):909-926. doi:10.1080/03639040701498759
  19. Teja SB, Patil SP, Shete G, Patel S, Bansal AK. Drug-excipient behavior in polymeric amorphous solid dispersions. *J Excipients Food Chem.* 2014;4(3):70-94.
  20. Melocchi A, Parietti F, Maroni A, Foppoli A, Gazzaniga A, Zema L. Hot-melt extruded filaments based on pharmaceutical grade polymers for 3D printing by fused deposition modeling. *Int J Pharm.* 2016;509(1-2):255-263. doi:10.1016/j.ijpharm.2016.05.036
  21. Palekar S, Nukala PK, Mishra SM, Kipping T, Patel K. Application of 3D printing technology and quality by design approach for development of age-appropriate pediatric formulation of baclofen. *Int J Pharm.* 2019;556(December 2018):106-116. doi:10.1016/j.ijpharm.2018.11.062
  22. Zhang J, Feng X, Patil H, Tiwari R V., Repka MA. Coupling 3D printing with hot-melt extrusion to produce controlled-release tablets. *Int J Pharm.* 2017;519(1-2):186-197. doi:10.1016/j.ijpharm.2016.12.049
  23. Korte C, Quodbach J. Formulation development and process analysis of drug-loaded filaments manufactured via hot-melt extrusion for 3D-printing of medicines. *Pharm Dev Technol.* 2018;23(10):1117-1127. doi:10.1080/10837450.2018.1433208
  24. Zhang J, Xu P, Vo AQ, et al. Development and evaluation of pharmaceutical 3D printability for hot melt extruded cellulose-based filaments. *J Drug Deliv Sci Technol.*

- 2019;52(April):292-302. doi:10.1016/j.jddst.2019.04.043
25. Dahl TC, Calderwood T, Bormeth A, Trimble K, Piepmeier E. Influence of physico-chemical properties of hydroxypropyl methylcellulose on naproxen release from sustained release matrix tablets. *J Control Release*. 1990;14(1):1-10. doi:10.1016/0168-3659(90)90055-X
  26. Viridén A, Wittgren B, Andersson T, Larsson A. The effect of chemical heterogeneity of HPMC on polymer release from matrix tablets. *Eur J Pharm Sci*. 2009;36(4-5):392-400. doi:10.1016/j.ejps.2008.11.003
  27. Tlegenov Y, Hong GS, Lu WF. Nozzle condition monitoring in 3D printing. *Robot Comput Integr Manuf*. 2018;54(April):45-55. doi:10.1016/j.rcim.2018.05.010
  28. Jain KK. Drug delivery systems - An overview. *Methods Mol Biol*. 2008;437:1-50. doi:10.1007/978-1-59745-210-6\_1
  29. Shimoni O, Postma A, Yan Y, et al. Macromolecule functionalization of disulfide-bonded polymer hydrogel capsules and cancer cell targeting. *ACS Nano*. 2012;6(2):1463-1472. doi:10.1021/nm204319b
  30. Willis L, Hayes D, Mansour HM. Therapeutic liposomal dry powder inhalation aerosols for targeted lung delivery. *Lung*. 2012;190(3):251-262. doi:10.1007/s00408-011-9360-x
  31. Staples M, Daniel K, Cima MJ, Langer R. Application of micro- and nano-electromechanical devices to drug delivery. *Pharm Res*. 2006;23(5):847-863. doi:10.1007/S11095-006-9906-4
  32. Vo AQ, Feng X, Morott JT, et al. A novel floating controlled release drug delivery system prepared by hot-melt extrusion. *Eur J Pharm Biopharm*. 2016;98:108-121. doi:10.1016/j.ejpb.2015.11.015

33. Paavola A, Kilpeläinen I, Yliruusi J, Rosenberg P. Controlled release injectable liposomal gel of ibuprofen for epidural analgesia. *Int J Pharm.* 2000;199(1):85-93. doi:10.1016/S0378-5173(00)00376-8
34. Santus G, Baker RW. Osmotic drug delivery: a review of the patent literature. *J Control Release.* 1995;35(1):1-21. doi:10.1016/0168-3659(95)00013-X
35. Leong KW, Langer R. Polymeric controlled drug delivery. *Adv Drug Deliv Rev.* 1988;1(3):199-233. doi:10.1016/0169-409X(88)90019-1
36. Kojima H, Yoshihara K, Sawada T, Kondo H, Sako K. Extended release of a large amount of highly water-soluble diltiazem hydrochloride by utilizing counter polymer in polyethylene oxides (PEO)/polyethylene glycol (PEG) matrix tablets. *Eur J Pharm Biopharm.* 2008;70(2):556-562. doi:10.1016/J.EJPB.2008.05.032
37. Bandari S, Nyavanandi D, Dumpa N, Repka MA. Coupling hot melt extrusion and fused deposition modeling: Critical properties for successful performance. *Adv Drug Deliv Rev.* 2021;172:52-63. doi:10.1016/j.addr.2021.02.006
38. Trenfield SJ, Awad A, Madla CM, et al. Shaping the future: recent advances of 3D printing in drug delivery and healthcare. <https://doi.org/101080/1742524720191660318>. 2019;16(10):1081-1094. doi:10.1080/17425247.2019.1660318
39. Sadia M, Arafat B, Ahmed W, Forbes RT, Alhnan MA. Channelled tablets: An innovative approach to accelerating drug release from 3D printed tablets. *J Control Release.* 2018;269:355-363. doi:10.1016/J.JCONREL.2017.11.022
40. Fina F, Goyanes A, Madla CM, et al. 3D printing of drug-loaded gyroid lattices using selective laser sintering. *Int J Pharm.* 2018;547(1-2):44-52. doi:10.1016/J.IJPHARM.2018.05.044

41. Isreb A, Baj K, Wojsz M, Isreb M, Peak M, Alhnan MA. 3D printed oral theophylline doses with innovative ‘radiator-like’ design: Impact of polyethylene oxide (PEO) molecular weight. *Int J Pharm.* 2019;564:98-105. doi:10.1016/J.IJPHARM.2019.04.017
42. Fina F, Madla CM, Goyanes A, Zhang J, Gaisford S, Basit AW. Fabricating 3D printed orally disintegrating printlets using selective laser sintering. *Int J Pharm.* 2018;541(1-2):101-107. doi:10.1016/J.IJPHARM.2018.02.015
43. Xu X, Robles-Martinez P, Madla CM, et al. Stereolithography (SLA) 3D printing of an antihypertensive polyprintlet: Case study of an unexpected photopolymer-drug reaction. *Addit Manuf.* 2020;33:101071. doi:10.1016/J.ADDMA.2020.101071
44. Khaled SA, Burley JC, Alexander MR, Yang J, Roberts CJ. 3D printing of five-in-one dose combination polypill with defined immediate and sustained release profiles. *J Control Release.* 2015;217:308-314. doi:10.1016/J.JCONREL.2015.09.028
45. Pereira BC, Isreb A, Forbes RT, et al. ‘Temporary Plasticiser’: A novel solution to fabricate 3D printed patient-centred cardiovascular ‘Polypill’ architectures. *Eur J Pharm Biopharm.* 2019;135:94-103. doi:10.1016/J.EJPB.2018.12.009
46. Melocchi A, Uboldi M, Parietti F, et al. Lego-Inspired Capsular Devices for the Development of Personalized Dietary Supplements: Proof of Concept With Multimodal Release of Caffeine. *J Pharm Sci.* 2020;109(6):1990-1999. doi:10.1016/j.xphs.2020.02.013
47. Melocchi A, Parietti F, Maccagnan S, et al. Industrial Development of a 3D-Printed Nutraceutical Delivery Platform in the Form of a Multicompartment HPC Capsule. *AAPS PharmSciTech.* 2018;19(8):3343-3354. doi:10.1208/s12249-018-1029-9
48. Okwuosa TC, Soares C, Gollwitzer V, Habashy R, Timmins P, Alhnan MA. On demand manufacturing of patient-specific liquid capsules via co-ordinated 3D printing and liquid

- dispensing. *Eur J Pharm Sci.* 2018;118:134-143. doi:10.1016/J.EJPS.2018.03.010
49. Liang K, Carmone S, Brambilla D, Leroux J-C. 3D printing of a wearable personalized oral delivery device: A first-in-human study. *Sci Adv.* 2018;4(5). doi:10.1126/SCIADV.AAT2544
50. Goyanes A, Det-Amornrat U, Wang J, Basit AW, Gaisford S. 3D scanning and 3D printing as innovative technologies for fabricating personalized topical drug delivery systems. *J Control Release.* 2016;234:41-48. doi:10.1016/j.jconrel.2016.05.034
51. Economidou SN, Pere CPP, Reid A, et al. 3D printed microneedle patches using stereolithography (SLA) for intradermal insulin delivery. *Mater Sci Eng C.* 2019;102:743-755. doi:10.1016/J.MSEC.2019.04.063
52. Melocchi A, Inverardi N, Ubaldi M, et al. Retentive device for intravesical drug delivery based on water-induced shape memory response of poly(vinyl alcohol): design concept and 4D printing feasibility. *Int J Pharm.* 2019;559:299-311. doi:10.1016/J.IJPHARM.2019.01.045
53. Geraili A, Janmaleki M, Sanati-Nezhad A, Mequanint K. Scalable microfabrication of drug-loaded core-shell tablets from a single erodible polymer with adjustable release profiles. *Biofabrication.* 2020;12(4):045007. doi:10.1088/1758-5090/AB97A0
54. Tan YJN, Yong WP, Kochhar JS, et al. On-demand fully customizable drug tablets via 3D printing technology for personalized medicine. *J Control Release.* 2020;322:42-52. doi:10.1016/J.JCONREL.2020.02.046
55. Chew SL, Mohac LM de, Raimi-Abraham BT. 3D-Printed Solid Dispersion Drug Products. *Pharm* 2019, Vol 11, Page 672. 2019;11(12):672. doi:10.3390/PHARMACEUTICS11120672

56. Goyanes A, Buanz ABM, Basit AW, Gaisford S. Fused-filament 3D printing (3DP) for fabrication of tablets. *Int J Pharm.* 2014;476(1-2):88-92. doi:10.1016/J.IJPHARM.2014.09.044
57. Goyanes A, Buanz ABM, Hatton GB, Gaisford S, Basit AW. 3D printing of modified-release aminosalicylate (4-ASA and 5-ASA) tablets. *Eur J Pharm Biopharm.* 2015;89:157-162. doi:10.1016/j.ejpb.2014.12.003
58. Basa B, Jakab G, Kállai-Szabó N, et al. Evaluation of biodegradable PVA-based 3D printed carriers during dissolution. *Materials (Basel).* 2021;14(6). doi:10.3390/ma14061350
59. Cheng Y, Qin H, Acevedo NC, Jiang X, Shi X. 3D printing of extended-release tablets of theophylline using hydroxypropyl methylcellulose (HPMC) hydrogels. *Int J Pharm.* 2020;591(October):119983. doi:10.1016/j.ijpharm.2020.119983
60. Xu F, Sun LX, Tan ZC, Liang JG, Zhang T. Adiabatic calorimetry and thermal analysis on acetaminophen. *J Therm Anal Calorim.* 2006;83(1):187-191. doi:10.1007/s10973-005-6969-0
61. Xu P, Li J, Meda A, et al. Development of a quantitative method to evaluate the printability of filaments for fused deposition modeling 3D printing. *Int J Pharm.* 2020;588(July):119760. doi:10.1016/j.ijpharm.2020.119760
62. Möckel JE, Lippold BC. Zero-Order Drug Release from Hydrocolloid Matrices. *Pharm Res* 1993 107. 1993;10(7):1066-1070. doi:10.1023/A:1018931210396
63. Tanigawara Y, Yamaoka K, Nakagawa T, Uno T. New Method for the Evaluation of in Vitro Dissolution Time and Disintegration Time. *Chem Pharm Bull.* 1982;30(3):1088-1090. doi:10.1248/CPB.30.1088
64. Windolf H, Chamberlain R, Quodbach J. Predicting drug release from 3D printed oral

- medicines based on the surface area to volume ratio of tablet geometry. *Pharmaceutics*. 2021;13(9). doi:10.3390/pharmaceutics13091453
65. Costa P, Sousa Lobo JM. Modeling and comparison of dissolution profiles. *Eur J Pharm Sci*. 2001;13(2):123-133. doi:10.1016/S0928-0987(01)00095-1
  66. Paarakh MP, Jose PANI, Setty CM, Peter G V. Release Kinetics – Concepts and Applications. *Int J Pharm Res Technol*. 2019;8(1):12-20. doi:10.31838/ijprt/08.01.02
  67. Siepmann J, Peppas NA. Modeling of drug release from delivery systems based on hydroxypropyl methylcellulose (HPMC). *Adv Drug Deliv Rev*. 2012;64(SUPPL.):163-174. doi:10.1016/J.ADDR.2012.09.028
  68. Peppas NA, Sahlin JJ. A simple equation for the description of solute release. III. Coupling of diffusion and relaxation. *Int J Pharm*. 1989;57(2):169-172. doi:10.1016/0378-5173(89)90306-2
  69. Dash S, Murthy PN, Nath L, Chowdhury P. Kinetic modeling on drug release from controlled drug delivery systems. *Acta Pol Pharm - Drug Res*. 2010;67(3):217-223.
  70. Rajisha KR, Deepa B, Pothan LA, Thomas S. Thermomechanical and spectroscopic characterization of natural fibre composites. *Interface Eng Nat Fibre Compos Maximum Perform*. Published online January 1, 2011:241-274. doi:10.1533/9780857092281.2.241
  71. Spink CH. Differential Scanning Calorimetry. *Methods Cell Biol*. 2008;84:115-141. doi:10.1016/S0091-679X(07)84005-2
  72. Gottschalk N, Bogdahn M, Harms M, Quodbach J. Brittle polymers in Fused Deposition Modeling: An improved feeding approach to enable the printing of highly drug loaded filament. *Int J Pharm*. 2021;597(October 2020):120216. doi:10.1016/j.ijpharm.2021.120216

73. Choiri S, Sulaiman TNS, Rohman A. Reducing Burst Release Effect of Freely Water-Soluble Drug Incorporated into Gastro-Floating Formulation Below HPMC Threshold Concentration Through Interpolymer Complex. *AAPS PharmSciTech*. 2019;20(5):1-11. doi:10.1208/s12249-019-1414-z
74. Goyanes A, Kobayashi M, Martínez-Pacheco R, Gaisford S, Basit AW. Fused-filament 3D printing of drug products: Microstructure analysis and drug release characteristics of PVA-based caplets. *Int J Pharm*. 2016;514(1):290-295. doi:10.1016/j.ijpharm.2016.06.021
75. O'donnell KL, Oporto-Velásquez GS, Comolli N. Evaluation of acetaminophen release from biodegradable poly (Vinyl alcohol) (PVA) and nanocellulose films using a multiphase release mechanism. *Nanomaterials*. 2020;10(2):11-14. doi:10.3390/nano10020301
76. Baggi RB, Babu N, Asian K. Calculation of predominant drug release mechanism using Peppas-Sahlin model, Part-I (substitution method): A linear regression approach. *Asian J Pharm Technol*. 2016;6(Dec):1-13.
77. Kikuchi A, Okano T. Pulsatile drug release control using hydrogels. *Adv Drug Deliv Rev*. 2002;54(1):53-77. doi:10.1016/S0169-409X(01)00243-5
78. Bussemer T, Otto I, Systems RB-DC, 2001 U. Pulsatile drug-delivery systems. *Crit Rev Ther Drug Carrier Syst*. 2001;18(5):433.
79. Santini JT, Richards AC, Scheidt R, Cima MJ, Langer R. Microchips as controlled drug-delivery devices. *Angew Chemie - Int Ed*. 2000;39(14):2396-2407. doi:10.1002/1521-3773(20000717)39:14<2396::AID-ANIE2396>3.0.CO;2-U
80. Prescott JH, Lipka S, Baldwin S, et al. Chronic, programmed polypeptide delivery from an implanted, multireservoir microchip device. *nature.com*. Published online 2006. doi:10.1038/nbt1199



81. Shidhaye S, Lotlikar V, Pharmacy AG-... R in, 2010 undefined. Pulsatile delivery systems: An approach for chronotherapeutic diseases. *sysrevpharm.org*. doi:10.4103/0975-8453.59513
82. Richards Grayson AC, Choi IS, Tyler BM, et al. Multi-pulse drug delivery from a resorbable polymeric microchip device. *nature.com*. Published online 2003. doi:10.1038/nmat998
83. reviews DF-A drug delivery, 2005 undefined. New oral delivery systems for treatment of inflammatory bowel disease. *Elsevier*. Accessed February 16, 2022. <https://www.sciencedirect.com/science/article/pii/S0169409X04001966>
84. Rathod SB, Bari MM, Barhate SD. PULSATILE DRUG DELIVERY SYSTEM: A REVIEW. *Swati al World J Pharm Res*. 2015;4. Accessed February 16, 2022. [https://wjpr.s3.ap-south-1.amazonaws.com/article\\_issue/1438324478.pdf](https://wjpr.s3.ap-south-1.amazonaws.com/article_issue/1438324478.pdf)
85. Jain D, Raturi R, Jain V, Bansal P, Singh R. Recent technologies in pulsatile drug delivery systems. *Biomatter*. 2011;1(1):57-65. doi:10.4161/biom.1.1.17717
86. Sungthongjeen S, Puttipipatkachorn S, Paeratakul O, Dashevsky A, Bodmeier R. Development of pulsatile release tablets with swelling and rupturable layers. *J Control Release*. 2004;95(2):147-159. doi:10.1016/j.jconrel.2003.10.023
87. Stanković M, Frijlink HW, Hinrichs WLJ. Polymeric formulations for drug release prepared by hot melt extrusion: application and characterization. *Drug Discov Today*. 2015;20(7):812-823. doi:10.1016/j.drudis.2015.01.012
88. Melocchi A, Parietti F, Loreti G, Maroni A, Gazzaniga A, Zema L. 3D printing by fused deposition modeling (FDM) of a swellable/erodible capsular device for oral pulsatile release of drugs. *J Drug Deliv Sci Technol*. 2015;30:360-367. doi:10.1016/J.JDDST.2015.07.016
89. Dumpa NR, Bandari S, Repka MA. Novel Gastroretentive Floating Pulsatile Drug Delivery

- System Produced via Hot-Melt Extrusion and Fused Deposition Modeling 3D Printing. *Pharm 2020, Vol 12, Page 52*. 2020;12(1):52. doi:10.3390/PHARMACEUTICS12010052
90. Melocchi A, Uboldi M, Briatico-Vangosa F, et al. The Chronotopic™ System for Pulsatile and Colonic Delivery of Active Molecules in the Era of Precision Medicine: Feasibility by 3D Printing via Fused Deposition Modeling (FDM). *Pharm 2021, Vol 13, Page 759*. 2021;13(5):759. doi:10.3390/PHARMACEUTICS13050759
91. Pimparade MB, Morott JT, Park JB, et al. Development of taste masked caffeine citrate formulations utilizing hot melt extrusion technology and in vitro-in vivo evaluations. *Int J Pharm*. 2015;487(1-2):167-176. doi:10.1016/j.ijpharm.2015.04.030
92. Amekyeh H, Tarlochan F, Billa N. Practicality of 3D Printed Personalized Medicines in Therapeutics. *Front Pharmacol*. 2021;12(April):1-15. doi:10.3389/fphar.2021.646836

# VITA

## PENGCHONG XU

### Education

M.S. in Pharmaceutical and Drug Delivery, University of Mississippi, USA 08/2016 - 05/2018

B.S. in Pharmacy, Shanghai University of Traditional Chinese Medicine, China 09/2012 - 07/2016

### Publications

- **Oral drug delivery systems using core-shell structure additive manufacturing technologies: a proof-of-concept study**  
Jiaxiang Zhang, Pengchong Xu, Anh Q Vo, Michael A Repka  
Journal of Pharmacy and Pharmacology, Volume 73, Issue 2, Pages 152–160.
- **Development of a quantitative method to evaluate the printability of filaments for fused deposition modeling 3D printing**  
Pengchong Xu, Jiangwei Li, Alvin Meda, Frederick Osei-Yeboah, Matthew L Peterson, Michael Repka, Xi Zhan  
International Journal of Pharmaceutics, Volume 588, Pages 119760.
- **A Novel Acetaminophen Soft-Chew Formulation Produced via Hot-Melt Extrusion with In-line Near-Infrared Monitoring as a Process Analytical Technology Tool**  
Pengchong Xu, Jiaxiang Zhang, Suresh Bandari, Michael A Repka  
AAPS PharmSciTech, Volume 21, Issue 2, Pages 1-10.
- **Development and evaluation of pharmaceutical 3D printability for hot melt extruded cellulose-based filaments**  
Jiaxiang Zhang, Pengchong Xu, Anh Q Vo, Suresh Bandari, Fengyuan Yang, Thomas Durig, Michael A Repka  
Journal of drug delivery science and technology, Volume 52, Pages 292.
- **Photostability Issues in Pharmaceutical Dosage Forms and Photo stabilization.**  
Janga, K.Y., King, T., Ji, N., Sarabu, S., Shadambikar, G., Sawant, S., Xu, P., Repka, M.A. and Murthy, S.N.  
AAPS PharmSciTech 19, 48–59 (2018). <https://doi.org/10.1208/s12249-017-0869-z>